This information is current as of January 6, 2021.

Antenatal Suppression of IL-1 Protects against Inflammation-Induced Fetal Injury and Improves Neonatal and Developmental Outcomes in Mice

Mathieu Nadeau-Vallée, Peck-Yin Chin, Lydia Belarbi, Marie-Ève Brien, Sheetal Pundir, Martin H. Berryer, Alexandra Beaudry-Richard, Ankush Madaan, David J. Sharkey, Alexis Lupien-Meilleur, Xin Hou, Christiane Quiniou, Alexandre Beaulac, Ines Boufaied, Amarilys Boudreault, Adriana Carbonaro, Ngoc-Duc Doan, Jean-Sebastien Joyal, William D. Lubell, David M. Olson, Sarah A. Robertson, Sylvie Girard and Sylvain Chemtob

J Immunol 2017; 198:2047-2062; Prepublished online 1 February 2017;
doi: 10.4049/jimmunol.1601600
http://www.jimmunol.org/content/198/5/2047

The Journal of Immunology is published twice each month by
The American Association of Immunologists, Inc.,
1451 Rockville Pike, Suite 650, Rockville, MD 20852

Print ISSN: 0022-1767 Online ISSN: 1550-6606.

Antenatal Suppression of IL-1 Protects against Inflammation-Induced Fetal Injury and Improves Neonatal and Developmental Outcomes in Mice

Mathieu Nadeau-Vallée,[*,†,‡,§] Peck-Yin Chin,[¶] Lydia Belarbi,[*,†,‡] Marie-Ève Brien,[‖,#] Sheetal Pundir,[*,†,‡,] Martin H. Berryer,[††] Alexandra Beaudry-Richard,[*,†,‡] Ankush Madaan,[*,†,‡,**] David J. Sharkey,[¶] Alexis Lupien-Meilleur,[††] Xin Hou,[*,†,‡] Christiane Quiniou,[*,†,‡] Alexandre Beaulac,[*,†,‡] Ines Boufaied,[‖,#] Amarilys Boudreault,[*,†,‡] Adriana Carbonaro,[‖,#] Ngoc-Duc Doan,[‡‡] Jean-Sebastien Joyal,[*,†,‡,§] William D. Lubell,[‡‡] David M. Olson,[§§,¶¶,‖‖] Sarah A. Robertson,[¶] Sylvie Girard,[‖,#] and Sylvain Chemtob[*,†,‡,§,**]**

Preterm birth (PTB) is commonly accompanied by in utero fetal inflammation, and existing tocolytic drugs do not target fetal inflammatory injury. Of the candidate proinflammatory mediators, IL-1 appears central and is sufficient to trigger fetal loss. Therefore, we elucidated the effects of antenatal IL-1 exposure on postnatal development and investigated two IL-1 receptor antagonists, the competitive inhibitor anakinra (Kineret) and a potent noncompetitive inhibitor 101.10, for efficacy in blocking IL-1 actions. Antenatal exposure to IL-1β induced *Tnfa*, *Il6*, *Ccl2*, *Pghs2*, and *Mpges1* expression in placenta and fetal membranes, and it elevated amniotic fluid IL-1β, IL-6, IL-8, and $PGF_{2\alpha}$, resulting in PTB and marked neonatal mortality. Surviving neonates had increased *Il1b*, *Il6*, *Il8*, *Il10*, *Pghs2*, *Tnfa*, and *Crp* expression in WBCs, elevated plasma levels of IL-1β, IL-6, and IL-8, increased IL-1β, IL-6, and IL-8 in fetal lung, intestine, and brain, and morphological abnormalities: e.g., disrupted lung alveolarization, atrophy of intestinal villus and colon-resident lymphoid follicle, and degeneration and atrophy of brain microvasculature with visual evoked potential anomalies. Late gestation treatment with 101.10 abolished these adverse outcomes, whereas Kineret exerted only modest effects and no benefit for gestation length, neonatal mortality, or placental inflammation. In a LPS-induced model of infection-associated PTB, 101.10 prevented PTB, neonatal mortality, and fetal brain inflammation. There was no substantive deviation in postnatal growth trajectory or adult body morphometry after antenatal 101.10 treatment. The results implicate IL-1 as an important driver of neonatal morbidity in PTB and identify 101.10 as a safe and effective candidate therapeutic. ***The Journal of Immunology*****, 2017, 198: 2047–2062.**

Preterm birth (PTB; birth at <37 wk of gestation) is a leading cause of infant mortality and morbidity worldwide and often results in lifelong complications for surviving children (1). Inflammation is implicated in a significant proportion of PTB regardless of the presence of infection (2) and is associated with the onset of fetal inflammatory response syndrome (FIRS) (3). Furthermore, inflammation represents an independent risk factor for neonatal morbidities (4–6). Increases in proinflammatory cytokines are readily detected in amniotic fluid and umbilical cord blood in such cases, and such increases herald the onset of neonatal morbidities (4, 7). Physiologically, cytokines in the fetal circulation rapidly spread and affect organs that are particularly vulnerable to inflammatory stressors at an early stage of development, especially in the premature newborn, by triggering intracellular signaling

*Department of Pediatrics, CHU Sainte-Justine Research Center, Montreal, Quebec H3T 1C5, Canada; †Department of Ophthalmology, CHU Sainte-Justine Research Center, Montreal, Quebec H3T 1C5, Canada; ‡Department of Pharmacology, CHU Sainte-Justine Research Center, Montreal, Quebec H3T 1C5, Canada; §Department of Pharmacology, University of Montreal, Montreal, Quebec H3T 1J4, Canada; ¶Department of Obstetrics and Gynecology, Adelaide Medical School and Robinson Research Institute, University of Adelaide, Adelaide, South Australia 5005, Australia; ‖Department of Obstetrics and Gynecology, University of Montreal, CHU Sainte-Justine Research Center, Montreal, Quebec H3T 1J4, Canada; #Department of Microbiology, Infectiology, and Immunology, University of Montreal, CHU Sainte-Justine Research Center, Montreal, Quebec H3T 1J4, Canada; **Department of Pharmacology and Therapeutics, McGill University, Montreal, Quebec H3G 1Y6, Canada; ††Department of Neurosciences, CHU Sainte-Justine Research Center, University of Montreal, Montreal, Quebec H3T 1J4, Canada; ‡‡Department of Chemistry, University of Montreal, Montreal, Quebec H3T 1J4, Canada; §§Department of Obstetrics and Gynecology, University of Alberta, Edmonton, Alberta T6G 2R3, Canada; ¶¶Department of Pediatrics, University of Alberta, Edmonton, Alberta T6G 2R3, Canada; and ‖‖Department of Physiology, University of Alberta, Edmonton, Alberta T6G 2R3, Canada

ORCIDs: 0000-0002-0923-0553 (P.-Y.C.); 0000-0002-5974-8916 (A.B.-R.); 0000-0002-4831-7950 (D.J.S.); 0000-0003-2735-3554 (A.L.-M.); 0000-0003-3877-9614 (J.-S.J.); 0000-0002-3080-2712 (W.D.L.).

Received for publication September 14, 2016. Accepted for publication December 30, 2016.

This work was supported by the Global Alliance for the Prevention of Prematurity and Stillbirth (an initiative of Seattle Children's) (to D.M.O., S.C., W.D.L., and S.A.R.), the SickKids Foundation–Canadian Institutes for Health Research (to S.G.), and by the Canadian Institutes for Health Research (to D.M.O., S.C., and S.A.R.). J.-S.J. is supported by the Burroughs Wellcome Fund Career Award for Medical Scientists, the Foundation Fighting Blindness, Fonds de Recherche du Québec en Santé, and by the Canadian Institutes for Health Research. M.N.-V. was supported by a Vanier Canada graduate scholarship, a scholarship from the Suzanne Veronneau-Troutman Funds associated with the Department of Ophthalmology of the University of Montreal, the Vision Research Network, Fonds de Recherche du Québec en Santé, and by the Canadian Institutes for Health Research. L.B. was supported by a scholarship from the National Sciences and Engineering Research Council of Canada. A.M. was a recipient of the Canadian Institutes for Health Research drug design training program and systems biology training program. M.-È.B. was supported by a scholarship from the Université de Montréal. M.H.B. was supported by a studentship from the Réseau de Médecine Génétique Appliquée and by a research award from the Department of Biomedical Sciences, University of Montreal. A. L.-M. was supported by a scholarship from the Canadian Institutes for Health Research. A.B.-R. was supported by a studentship from the Fondation de l'Hôpital Maisonneuve-Rosemont. S.C. holds a Canada Research Chair (Vision Science) and the Leopoldine Wolfe Chair in translational research in age-related macular degeneration.

(Continued on next page)

cascades that result in organ injuries and neonatal morbidity (8, 9), with vulnerability primarily observed in lung, intestine, and brain (10–13). Correspondingly, key features of tissue (lung, gut, and brain) injury of common neonatal diseases can be reproduced in animals following administration of inflammatory stressors (14–16); conversely, tissue integrity can be preserved by anti-inflammatory agents (17–19). Despite this compelling evidence and the unequivocal need to tackle inflammation to treat PTB and neonatal injury (20), currently available treatments for preterm labor, so-called tocolytics only tackle myometrial contractions and have no impact on the inflammatory mediators implicated in fetal inflammatory injury.

To date, there is no therapeutic molecule available to prevent/alleviate pathological inflammatory processes in pregnant women at risk for PTB. Of all mediators implicated in gestational inflammation and the onset of neonatal morbidities, IL-1, which is a potent pleiotropic cytokine central to numerous inflammatory processes and capable of mounting an acute inflammatory response via ubiquitously expressed IL-1R, exerts a major detrimental role, as suggested by a broad body of evidence, including: 1) increased levels of IL-1β and IL-1Ra are early markers of neonatal injuries of the lung, intestine, and brain (21–24), and such injuries can be recreated in rodent and ovine models via overexpression or administration of IL-1 (25–27); 2) antagonism of the IL-1 receptor, IL-1β, or inhibition of the cleavage and release of IL-1β by targeting caspase-1 activity provides improvement in outcomes of perinatal injuries to the aforementioned organs, including when triggered by upstream proinflammatory stressors (17, 19, 28–32); and 3) inflammatory concentrations of IL-1β elicit neuromicrovascular decay (33), curtail hippocampal neuron differentiation (34), and consequently lead to seizures wherein IL-1β further contributes to brain injury (35). Therefore, IL-1 represents a target of high interest and potential to improve health outcomes in premature infants. However, data accumulated to date mainly describe a harmful role of IL-1 in the postnatal period, whereas its antenatal contribution to neonatal diseases is not well described, which hinders the development of a therapeutic administered preferably during pregnancy at the onset of chorioamnionitis. This is particularly relevant considering that IL-1β levels are elevated in women with chorioamniotis (36), which constitutes an early event in the onset of perinatal complications in humans and animals (37–39), and that administration of IL-1β in pregnant rodents and nonhuman primates induces PTB (40–43).

Therefore, we sought to investigate the effects exerted by antenatal exposure to IL-1β on the development of offspring. We focused on changes induced by intrauterine exposure to IL-1β, particularly in the placenta, fetal membranes, and amniotic fluid, and its association with the onset of a fetal inflammatory response and gestation outcome. Furthermore, we studied litters postnatally to assess growth and development of surviving offspring, with specific consideration of the morphology of lung parenchyma and intestinal villi, as well as microvascular development in brain and normal cortex function, which are cardinal features of common neonatal morbidities. To evaluate the utility of suppressing IL-1 signaling to protect the fetus from inflammatory injury, we used a commercially available IL-1R competitive antagonist anakinra (Kineret), in addition to a small peptide noncompetitive IL-1R antagonist (termed 101.10) (44) that has proven effective at decreasing IL-1–induced uterine inflammation in pregnant mice via inhibition of IL-1–induced MAPK p38 and JNK, c-jun, and Rho GTPase (42) upstream of transcription factor AP-1 implicated in cytokine induction (45–47) and labor (48). Our data in IL-1β– and LPS-induced models of PTB uncover a major detrimental role of antenatal IL-1 on the development of adverse perinatal, neonatal, and developmental outcomes in progeny, and they suggest that 101.10 represents an effective therapeutic candidate for administration preferably during pregnancy to decrease neonatal morbidities, including in cases of infection.

Materials and Methods

Animals

IL-1β model. Timed-pregnant CD-1 mice were obtained from Charles River Laboratories at different gestation ages and were allowed to acclimatize for 4 d prior to experiments. Animal studies were approved by the Animal Care Committee of Hôpital Sainte-Justine along the principles of the *Guide for the Care and Use of Experimental Animals* of the Canadian Council on Animal Care. The animals were maintained on standard laboratory chow under a 12:12 h light/dark cycle and allowed free access to chow and water.

LPS model. C57BL/6 (B6) mice were bred and housed in the specific pathogen-free University of Adelaide Laboratory Animal Services facility under a 12:12 h light/dark cycle. Food and water were provided ad libitum. Animals were used in accordance with the National Health and Medical Research Council Australian Code of Practice for the care and use of animals for scientific purposes, and all experiments were approved by the University of Adelaide Animal Ethics Committee. One to three virgin female mice of 8–12 wk of age were housed with a proven fertile B6 male and checked daily between 8:00 and 10:00 AM for vaginal plugs, as evidence of mating. The morning of vaginal plug detection was designated gestational day (GD)0.5. Females were then removed from the male and housed individually. Data presented in this study using B6 mice are concordant with those previously reported with CD-1 mice (42).

Chemicals

Chemicals were purchased from the following manufacturers: recombinant human IL-1β (PeproTech, no. 200-01B), LPS from *Salmonella typhimurium* (Sigma-Aldrich, St. Louis, MO), 101.10 [Elim Biopharmaceuticals, Hayward, CA; and synthetized as previously reported (49, 50)], and Kineret (Swedish Orphan Biovitrum, Stockholm, Sweden).

IL-1β–induced PTB model

Timed-pregnant CD-1 mice were steadily anesthetized with an isoflurane mask for the complete procedure. After body hair removal from the peritoneal area, a 1.5-cm medial incision was performed with surgical scissors in the lower abdominal wall. The lower segment of the right uterine horn was exposed and 1 μg of IL-1β was injected between two fetal membranes with care to not enter the amniotic cavity. The abdominal muscle layer was sutured and the skin closed with clips. One hundred microliters of 101.10 (1 mg/kg per 12 h), Kineret (4 mg/kg per 12 h), or vehicle was injected s.c. in the neck 30 min before stimulation with IL-1β. Time of parturition and newborn outcome was assessed every 2 h until term (GD19–GD19.5). A subset of pregnant mice was sacrificed 24 h after the IL-1β injection to collect fluid and tissue samples of amniotic fluids, fetal membranes and placenta for biochemical analysis, and fetuses for gross fetal growth assessment. Another subset was killed immediately after delivery (±2 h postpartum), and samples of brain, lung, intestine, and WBCs (as described

(*Continued from page 1*)

M.N.-V, S.P., S.A.R., S.G., and S.C. designed the research studies; M.N.-V., P.-Y.C., L.B., M.-È.B., S.P., M.H.B., A.M., A.B.-R., D.J.S., A.L.-M., X.H., A. Boudreault, A.C., I.B., and S.G. conducted experiments; M.N.-V., P.-Y.C., L.B., M.-È.B., S.P., M.H.B., A.M., A.B.-R., X.H., and S.G. analyzed data; W.D.L. and N.-D.D. provided reagents; and M.N.-V., A.B.-R., C.Q., J.-S.J., A. Beaulac, D.M.O., S.A.R., S.G., and S.C. wrote or contributed to the writing of the manuscript.

Address correspondence and reprint requests to Dr. Sylvain Chemtob, Dr. Sylvie Girard, or Dr. Sarah A. Robertson, CHU Sainte-Justine, Research Center, Departments of Pediatrics, Ophthalmology, and Pharmacology, 3175 Chemin Côte Ste-Catherine, Montreal, QC H3T 1C5, Canada (S.C.), CHU Sainte-Justine, Research Center, Departments of Obstetrics and Gynecology, 3175 Chemin Côte Ste-Catherine, Montreal, QC H3T 1C5, Canada (S.G.), or Robinson Research Institute and Adelaide Medical School, University of Adelaide, Adelaide, SA 5005, Australia (S.A.R.). E-mail addresses: sylvain.chemtob@umontreal.ca (S.C.), sylvie.girard@recherche-ste-justine.qc.ca (S.G.), or sarah.robertson@adelaide.edu.au (S.A.R.)

The online version of this article contains supplemental material.

Abbreviations used in this article: B6, C57BL/6; BPD, bronchopulmonary dysplasia; FIRS, fetal inflammatory response syndrome; GD, gestational day; NEC, necrotizing enterocolitis; PT, postterm day; PTB, preterm birth; VEP, visual evoked potential.

below) were collected and stored at −80°C for biochemical analysis. Pups (up to eight per litter) were kept with dams and weighed every 2–3 d, then killed on postterm day (PT)15 (representing adolescent pups in terms of brain development) and PT30 (at the stage of young adulthood in terms of brain development) for further histological and electrophysiological analysis, respectively.

Circulating leukocyte RNA isolation

Newborn blood was collected by decapitation, pooled together for each litter, and immediately transferred into heparin-containing tubes to prevent clotting. WBCs were isolated by centrifugation after a treatment with RBC lysis buffer (Norgen Biotek, Thorold, ON, Canada) and EDTA according to the manufacturer's protocol, and the resulting pellets were stored at −80°C. For RNA isolation, pellets were thawed, lysed, and passed through an RNA-binding column using a leukocyte RNA isolation kit according to the manufacturer's protocol (Norgen Biotek). Briefly, after washing, RNA was eluted from the columns and quantified with using a NanoDrop 1000 spectrophotometer. Equal amounts of RNA were used to synthetize cDNA using iScript reverse transcription supermix (Bio-Rad Laboratoties, Hercules, CA). Real-time quantitative PCR was then performed on the samples as described below.

RNA extraction and real-time quantitative PCR

Tissues were thawed and rapidly preserved in Ribozol (Amresco, Solon, OH). RNA was extracted according to the manufacturer's protocol and samples were DNAse treated using an Ambion DNA-free kit according to the manufacturer's instructions. RNA concentration and integrity were measured with a NanoDrop 1000 spectrophotometer, and samples with an absorbance at 260/280 nm ratio of 1.6–1.8 were used in PCR analysis after RNA integrity was verified by denaturing agarose electrophoresis. Five hundred nanograms of RNA was used to synthetize cDNA using iScript reverse transcription superMix (Bio-Rad Laboratories). Primers were designed using National Center for Biotechnology Information Primer Blast (see Table II). Quantitative gene expression analysis was performed on an MXPro3000 (Stratagene) with SYBR Green master mix (Bio-Rad Laboratories). PCR products were subjected to high-resolution melt analysis to assess primer specificity. Gene expression levels were normalized to 18S universal primer (Ambion/Life Technologies, Burlington, ON, Canada) or β-actin.

Murine ELISAs

The ELISAs were performed using the following ELISA kits according to the manufacturers' protocols: mouse IL-1β/IL-1F2 Quantikine (R&D Systems, no. MLB00C), mouse IL-6 Quantikine (R&D Systems, no. M6000B), mouse IL-8 (MyBioSource, no. MBS261967; recognizes the IL-8 homolog CXCL2), and mouse $PGF_{2\alpha}$ (MyBioSource, no. MBS264160). Briefly, tissues were lysed in RIPA buffer (containing proteases inhibitors) and equal amounts of proteins (assessed using Bradford method) or 50 μl of fetal plasma or amniotic fluids was loaded into a 96-well plate precoated with specific primary Abs and incubated for 2 h at ambient temperature. Wells were then washed five times and incubated with enzyme-linked polyclonal secondary Abs for 2 h. After another washing step, a substrate solution was added. The enzymatic reaction was stopped after 30 min and plates were read at 450 nm, with wavelength correction set to 570 nm.

Western blotting

Proteins from homogenized placenta lysed in RIPA buffer (containing proteases inhibitors) were quantified using Bradford's method (Bio-Rad Laboratories). Fifty micrograms of protein sample was loaded onto SDS-PAGE gel and electrotransfered onto polyvinylidene difluoride membranes. After blocking, membranes were incubated with either an Ab against phospho-JNK (Cell Signaling Technology, Whitby, ON, Canada, no. 9251), IL-6 (Santa Cruz Biotechnology, no. sc-1264), or β-actin (Santa Cruz Biotechnology, no. sc-47778). Membranes were then washed with PBS containing 0.1% Tween 20 (Sigma-Aldrich) and incubated for 1 h with their respective secondary Abs conjugated to HRP (Sigma-Aldrich). ECL (GE Healthcare) was used for detection using the ImageQuant LAS 500 (GE Healthcare, Little Chalfont, U.K.), and densitometric analysis was performed using ImageJ (National Institutes of Health; http://rsb.info.nih.gov/ij/). Resulting values were normalized first with β-actin, and then as a ratio of the control samples.

Tissue collection and fixation

Pups were sacrificed at PT15, intubated via the trachea, and perfused with 10% formalin (Fisher Scientific) at a pressure of 20 cm. After 10 min, lung, intestine, and brain were collected. Briefly, the cranium was opened with surgical scissors (following the sagittal suture from sigma to bregma) and the brain was carefully extracted. Then, the lower intestine (1 cm above the cecum to the rectum) and lungs were excised and all tissues were fixed in 10% formalin for at least 24 h and subsequently transferred to PBS at 4°C.

Lung, intestine, and brain histology

Five micrometer–thick sections were performed on paraffin-embedded lungs (at three levels from the apex to base), intestines (ileum to colon), and brains and stained with H&E (lungs and brains) or hematoxylin/phloxine/safran (intestine). Images were acquired using a ×20 objective with a high-resolution slide scanner (Axio Scan; Zeiss, North York, ON, Canada).

Histological analysis

Analyses were performed with Zen2 software or ImageJ by evaluators blinded to group identification. Tissues were obtained from 2 pups per dam from 6 to 8 dams per group (total of 28 dams and 56 pups). A postanalysis was performed to determine whether the morphological differences observed were dependent on the sex of pups; no significant differences were noted (data not shown).

Lung. Alveolar count was obtained from the mean of two 1-mm^2 sections in each tissue section analyzed. Alveolar size and parenchymal thickness were obtained from the mean of 10 alveoli per tissue section from two different areas. The number of intercepts between a 1-mm straight line (generated with Zen2 software) and lung structure was used as an index of alveolar counts (51). The results are presented as an absolute number per millimeter of the mean from four separate 1-mm^2 sections that were free of blood vessels.

Intestine. Villus height was measured from the basal layer of the submucosa to the ending of the villus in the jejunum–ileum; atrophied villi were arbitrarily defined as villi measuring <400 μm, which corresponds to a 2-fold decrease in mean villus height of controls at the same age. In colon, lymphoid follicle count was divided by the length of the tissue analyzed and plotted as count per millimeter. The surface of lymphoid follicles was measured on all follicles encountered.

Brain. Immunohistochemistry was performed as previously described (52). Immunostaining for lectin (vasculature, shown in brown) was separated from the purple hematoxylin using the color deconvolution function in ImageJ, and staining density was determined using ImageJ analysis software as previously described (53). Staining threshold was then set to detect only specific lectin staining and then applied to all samples, allowing semi-quantitative comparisons of the vascular density.

Immunocytochemistry

Pregnant mice (GD17) injected s.c. with 1 mg/kg 101.10-FITC, FITC alone (Sigma-Aldrich), or vehicle were euthanized after 1 h to analyze tissue distribution of the fluorescent-tagged compounds. Placentas and fetuses were collected and fixed in 4% paraformaldehyde for 1 d and transferred in 30% sucrose for another day. Localization of 101.10 was determined on 14-μm longitudinal placenta and fetus cryosections. Nuclei were stained with DAPI (1:5000; Invitrogen). Images of the complete sections were captured using a ×10 objective with an Axio Observer.Z1 (Zeiss, San Diego, CA) and merged into a single file using the MosaiX option in the AxioVision software version 4.6.5 (Zeiss).

Flow cytometry

Samples were lysed and filtered to obtain a single-cell suspension and then analyzed on a BD FACSAria flow cytometer (BD Biosciences) equipped with 488-, 405-, and 633-nm lasers and routinely calibrated with CS&T beads (BD Biosciences). Data were processed using BD FACSDiva (BD Biosciences), and detection of FITC emission was collected through a 530/30 band pass filter. A minimum of 10,000 total events were acquired for each sample. Data analysis was performed with FlowJo software (Tree Star, Ashland, OR), and results were reported as a percentage of positive cells in the tested sample.

Visual evoked potential

Visual evoked potential (VEP) is a reliable and sensitive parameter to evaluate neurologic functional alterations. VEPs were recorded at PT30. Mice were anesthetized using a mixture of 80 mg/kg ketamine and 20 mg/kg xylazine. A s.c. needle electrode (Diagnosys) was inserted under the scalp at the lambda suture and served as the active electrode, whereas reference and ground electrodes (Diagnosys) were placed in the cheek and tail, respectively. Impedance was maintained at <5 kΩ. Visual stimuli were generated by a Mini-Ganzfeld stimulator (3 cd·s/m^2). Flash VEPs were elicited by a brief flash (≤5 ms) in the visual field presented in a dark room (red light) without prestimulus. Analog high-pass and low-pass filters were set at ≤1 Hz and at ≥100 Hz, respectively. Photic stimulation was delivered 100 times at a frequency of 1 Hz. The robust components of flash VEPs are N2 and P2 peaks. Measurement of P2 amplitude was made from positive P2 peak and

preceding N2 negative peak. Each response represents an average of 100 sweeps (performed with Espion E^3 systems).

LPS-induced PTB model, progeny growth trajectory, and body composition

B6 pregnant mice at GD16.5 were injected with 101.10 (1 mg/kg) or vehicle i.p. 30 min prior to injection of 0.5 μg of LPS in 200 μl of PBS. Mice were then administered additional doses of 101.10 or vehicle on GD17.0, GD17.5, and GD18.0. A subset of pregnant females was killed by cervical location 4 h posttreatment, and the uterus, decidua, placenta, and fetal brain were dissected from two fetuses (one from each horn), snap frozen in liquid nitrogen, and stored at −80°C for mRNA isolation. Another cohort of female mice was monitored until the time of parturition. Gestation length and the number of pups were recorded. Viable pups were weighed within the first 24 h of life. Pups were then sexed at weaning (3 wk of age) when they were weighed again. All offspring were weighed at 4 wk of age and then every 2 wk until 20 wk of age. At 20 wk, progeny were anesthetized (tribromoethanol [Avertin]; Sigma-Aldrich) and ∼1 ml of blood was collected by cardiac puncture before mice were weighed and killed by cervical dislocation for full-body composition analysis. The following tissues were excised and weighed individually: brain, heart, lungs (left and right), kidneys (left and right), liver, adrenal glands (left and right), thymus, spleen, testes (males, left and right), seminal vesicle (males), epididymis (males), ovaries (females, left and right), uterus (females), quadriceps (left and right), triceps (left and right), biceps (left and right), gastrocnemius muscle (left and right), retroperitoneal fat, perirenal fat, epididymal fat (males, left and right), and parametrial fat (females). Weights of tissues and organs present on both the left and right sides were summed. Total muscle weight was calculated by adding the combined weights of the quadriceps, triceps, and biceps and gastrocnemius muscles. Total fat weight was calculated by adding the combined weights of the retroperitoneal fat, perirenal fat, and epididymal fat (for males) or parametrial fat (for females). Total muscle and total fat weights were used to calculate the muscle/fat ratio. Total fat weight was subtracted from total body weight to calculate the total lean weight.

Serum preparation

Immediately following collection, serum was prepared by first allowing blood to clot at room temperature for 30 min, and then serum was separated by centrifugation at 4000 rpm for 5 min, removed, and divided into small individual aliquots to avoid multiple freeze/thaw cycles. Serum aliquots were immediately stored at −80°C until assay.

Mouse Luminex assays

Adiponectin and leptin were quantified by a Luminex multiplex microbead assay (Millipore, Bayswater, VIC, Australia), according to the manufacturer's instructions. For adiponectin, serum samples were diluted 1 in 5000 in assay buffer, as recommended by the manufacturer, whereas for leptin, samples were tested neat. The minimum detectable threshold was 3.0 pg/ml and 4.2 pg/ml for adiponectin and leptin, respectively.

Statistical analysis

All data were analyzed using SPSS version 20.0 software (SPSS, Chicago, IL) or GraphPad Prism version 6.0 software (GraphPad Software, San Diego, CA). Groups were tested for normality using a Shapiro–Wilk test. A one-way ANOVA or two-tailed Student *t* test was employed when data were normally distributed. A Dunnett multiple comparison method was used when data were compared with a single control. A Kruskal–Wallis test followed by a Mann–Whitney *U* test was used when the data were not normally distributed. Body composition data are expressed as estimated marginal mean ± SEM and analyzed as a mixed model linear repeated measures ANOVA and with a post hoc Sidak test, with litter size as a covariant. A p value < 0.05 was considered statistically significant. Data are presented as means ± SEM for large sample size and individual values plus median for small sample sizes.

Results

Administration of IL-1β in utero induces adverse perinatal outcomes

To study the implications of antenatal exposure to IL-1β, we administered IL-1β intrauterine in late gestation (GD16; normal gestation length, 19.5 d) (Fig. 1A) to induce uterine inflammation and preterm delivery (42, 54). IL-1R competitive antagonist Kineret and noncompetitive IL-1R antagonist (small all-D peptide) 101.10 (44) were administered s.c. to additional groups of IL-1β–treated dams twice daily from GD16 to GD18. IL-1β shortened gestation length (Fig. 1B) and induced substantial neonatal mortality (Fig. 1C, 1D), whereas coadministration of 101.10, but not Kineret, significantly improved these outcomes. Most pups alive after birth survived the first week of life in all treatment groups (Fig. 1E).

Given the high neonatal mortality rate, we examined the fetal response to IL-1β by conducting gross and histological examination of fetuses after 24 h of exposure to IL-1β in utero. We found that most fetuses from IL-1β–treated dams displayed an underdeveloped anatomy in addition to noticeable autolysis (Fig. 1F, arrows). In contrast, none of these features was observed in fetuses from IL-1β–treated dams receiving 101.10, in line with improved neonatal survival as previously described (see Fig. 1C). In fetuses that developed normally, no significant difference in morphological parameters between groups was found after 24 h exposure to IL-1β in utero, as measured by histological analysis (Fig. 1G, Table I). Correspondingly, the weight of viable newborns was not significantly different between groups (Fig. 1H), suggesting that short-term exposure to (nonlethal) inflammation is insufficient to affect late prenatal growth, although a slight tendency is observed for weight.

Uterine IL-1β induces an inflammatory response in placenta, fetal membranes, and amniotic fluids that propagates to newborn

To characterize the maternal and fetal inflammatory response triggered by IL-1β in pregnant uterus and to further explore the link between maternal-onset inflammation and the adverse perinatal outcomes observed in this study, we performed biochemical analysis on fetal–maternal tissues (placenta, fetal membranes, and amniotic fluids collected 24 h after IL-1β injection) of normally developed fetuses (see Fig. 1F–H, Table I). Placental expression of genes encoding key proinflammatory factors (Table II), including TNF-α, IL-6, CCL2, and Cox-2, was upregulated in IL-1β–treated dams (Fig. 2A). This upregulation was blocked by 101.10, which is readily able to access the placenta (Supplemental Fig. 1A–D), and to a lesser extent Kineret as previously reported for other inflammatory genes, including *Il1b* and *Il8* (42); anti-inflammatory IL-10 and IL-4 were unaffected by IL-1β in the absence or presence of 101.10 or Kineret (Fig. 2A). The strong induction of placental *Il6* by IL-1β (and its downregulation by 101.10) was reflected in protein abundance (Fig. 2B) and was associated with activation (by phosphorylation) of the IL-1R–induced stress kinase JNK (Supplemental Fig. 2A). A similar proinflammatory profile was observed in fetal membranes (Supplemental Fig. 2B). Furthermore, proinflammatory mediators associated with parturition (IL-1β, IL-6, IL-8, and $PGF_{2\alpha}$) in amniotic fluids were concurrently elevated in IL-1β–treated dams (Fig. 2C–F), suggesting propagation of the initial inflammatory response into the fetal compartment as expected (3, 55). Again, 101.10 blocked this effect with more efficacy than Kineret (at recommended doses, effective on maternal inflammation) (42). The inefficacy of Kineret on fetal–placental inflammation was dose related, as higher doses reduced inflammation and PTB (Supplemental Fig. 2C–E).

To confirm dissemination of maternal inflammation to the fetus, we quantified proinflammatory mRNAs and proteins in WBCs and plasma of neonates (collected within an hour of birth). A significant increase in *Il1b*, *Il6*, *Il8*, *Il10*, *Pghs2*, *Tnfa*, and *Crp* was observed in circulating WBCs (Fig. 2G), associated with elevated levels of IL-1β, IL-6, and IL-8 in plasma (Fig. 2H–J). Again, 101.10 abrogated this increase with higher efficacy than Kineret. Notably, FITC-coupled 101.10 was not detectable in fetal tissues when administered s.c. to dams (Supplemental Fig. 1E–I), suggesting

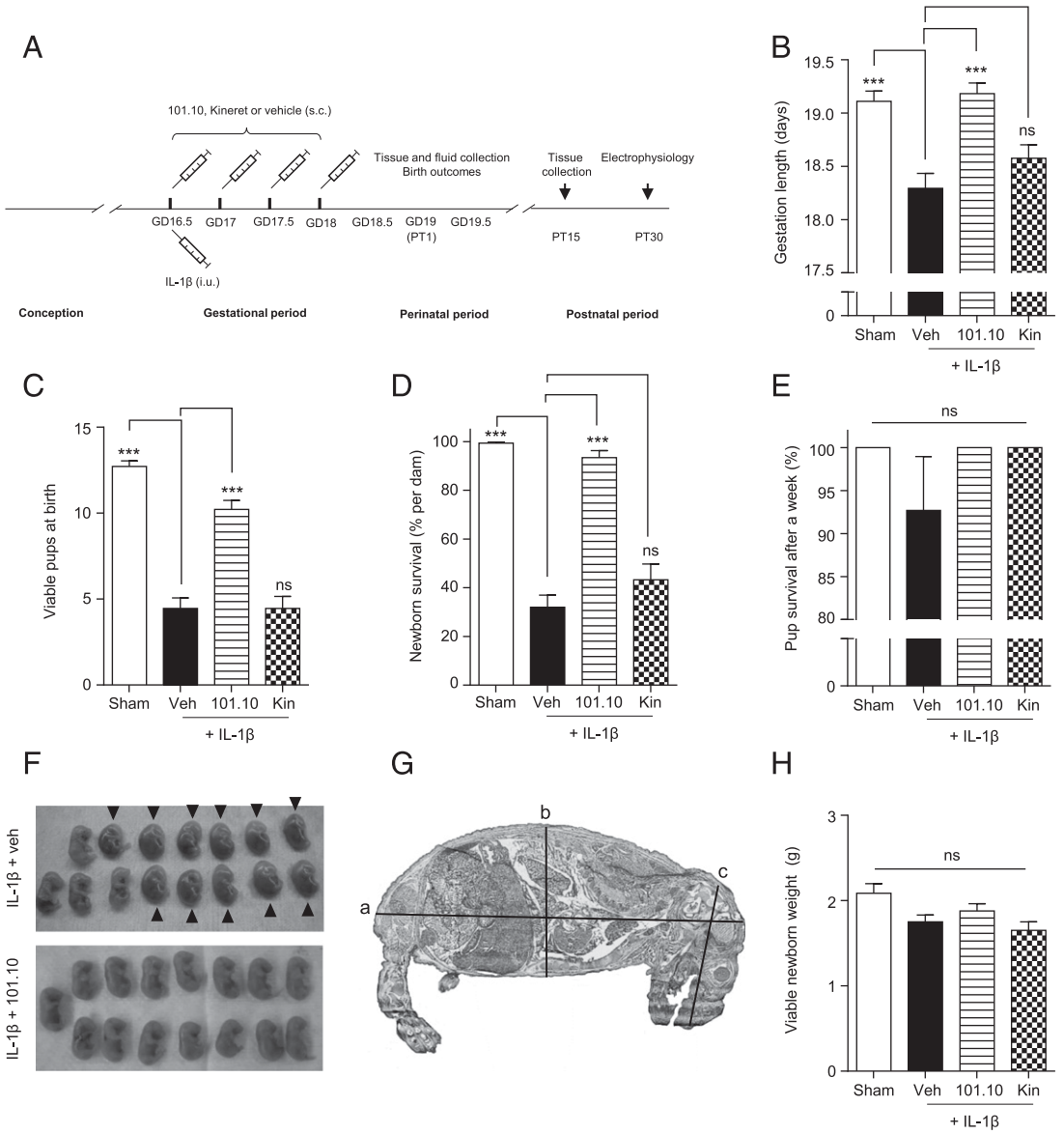

FIGURE 1. Adverse gestational and perinatal outcomes are induced by antenatal exposure to IL-1β and corrected by 101.10. (**A**) 101.10 (1 mg/kg per 12 h), Kineret (4 mg/kg per 12 h), or vehicle are administered s.c. for 2 consecutive days and IL-1β (1 μg) is administered intrauterine at GD16.5. (**B**–**D**) Gestation length (B), viable pup count (C), and pup survival rate as determined by counting breathing and nonbreathing pups at birth (D). (**E**) Pup survival rate at 1 wk (denominator is viable pups at birth). (**F**) Representative images of late gestation fetuses recovered from dams administered IL-1β with or without 101.10, analyzed after autopsy at GD17.5 (24 h after intrauterine IL-1β injection). Pups displaying gross morphological or developmental anomalies are indicated with arrowheads. (**G**) Representative micrograph of the morphology measurements (shown in Table I) in a normally developed pup at GD17.5. (**H**) Pup weight at 24 h postbirth. n = 18–50 dams per group for gestational and neonatal outcome data, and 8–15 dams per group for postbirth data. Values are presented as means ± SEM. ***$p < 0.001$ by one-way ANOVA with a Dunnett postanalysis.

that its protective effects on the fetus may be mediated via suppression of gene expression in placenta and gestational tissue, as opposed to direct suppression of IL-1β signaling within the fetus (see Fig. 2A, 2B, Supplemental Figs. 1A–D, 2A, 2B).

Given the strong elevation in plasma cytokines IL-1β, IL-6, and IL-8 in newborns exposed to IL-1β in utero, we assessed whether the lung, intestine, and brain, which are well-perfused organs particularly vulnerable to inflammatory insults (10–13), were affected

Table I. Body morphometry in fetuses 24 h after exposure to IL-1β and vehicle, 101.10, or Kineret

	Sham (n = 4)	IL-1β + Vehicle (n = 4)	IL-1β + 101.10 (n = 4)	IL-1β + Kineret (n = 4)
Head length (μm)	7,078 ± 148	7,405 ± 293	7,498 ± 115	7,176 ± 293
Body length (μm)	20,535 ± 194	20,587 ± 764	20,658 ± 438	20,217 ± 694
Thorax length (μm)	5,623 ± 334	5,889 ± 436	5,824 ± 238	5,677 ± 238

All data are presented as estimated marginal means ± SEM and analyzed using one-way ANOVA with a Dunnett multiple comparison test. Differences between treatment and control groups are considered significant when $p < 0.05$.

Table II. Primers for mRNA expression analysis

Gene	Forward and Reverse Primer Sequences	GenBank Accession No.
Il1a	F-5′-CCGACCTCATTTTCTTCTGG-3′ R-5′-GTGCACCCGACTTTGTTCTT-3′	NM_010554.4
Il1b	F-5′-CCAAAGCAATACCCAAAGAAA-3′ R-5′-GCTTGTGCTCTGCTTGTGAG-3′	NM 008361.3
Il1b (second pair)	F-5′-AGATGAAGGGCTGCTTCCAAA-3′ R-5′-GGAAGGTCCACGGGAAAGAC-3′	NM 008361.3
Il4	F-5′-CCATATCCACGGATGCGACA-3′ R-5′-CTGTGGTGTTCTTCGTTGCTG-3′	NM 021283
Il6	F-5′-ACAACCACGGCCTTCCCTAC-3′ R-5′-TCCACGATTTCCCAGAGAACA-3′	NM 031168.1
Il6 (second pair)	F-5′-CAACGATGATGCACTTGCAGA-3′ R-5′-TCTCTCTGAAGGACTCTGGCT-3′	NM 031168.1
Il10	F-5′-AGGCGCTGTCATCGATTTCT-3′ R-5′-TGGCCTTGTAGACACCTTGGT-3′	NM 010548.2
Il10 (second pair)	F-5′-TAACTGCACCCACTTCCCAG-3′ R-5′-AGGCTTGGCAACCCAAGTAA-3′	NM 010548.2
Il12b	F-5′-TGACACGCCTGAAGAAGA-3′ R-5′-AGAGACGCCATTCCACAT-3′	NM 008352.2
Il12b (second pair)	F-5′-TGGGAGTACCCTGACTCCTG-3′ R-5′-AGGAACGCACCTTTCTGGTT-3′	NM 008352.2
Tnf	F-5′-GTAGCCCACGTCGTA-3′ R-5′-TCCACGATTTCCCAG-3′	NM 013693.3
Tnf (second pair)	F-5′-GCCTCTTCTCATTCCTGCTTG-3′ R-5′-CTGATGAGAGGGAGGCCATT-3′	NM 013693.3
Actb	F-5′-CGTGGGCCGCCCTAGGCACCA-3′ R-5′-ACACGCAGCTCATTGTA-3′	NM 007393.3
Crp	F-5′-TCTGCACAAGGGCTACACTG-3′ R-5′-ATCTCCGATGTCTCCCACCA-3′	NM 007768
Pghs2	F-5′-ACCTCTCCACCAATGACCTGA-3′ R-5′-CTGACCCCCAAGGCTCAAAT-3′	NM_011198.4
Ccl2	F-5′-GCTCAGCCAGATGCAGTTA-3′ R-5′-TGTCTGGACCCATTCCTTCT-3′	NM_011333
Ccl3	F-5′-CCCAGCCAGGTGTCATTTTC-3′ R-5′-GTGGCTACTTGGCAGCAAAC-3′	NM_011337.2
Mpges1	F-5′-GCTGCGGAAGAAGGCTTTTG-3′ R-5′-GGTTGGGTCCCAGGAATGAG-3′	NM_022415

F, forward; R, reverse.

by the systemic inflammatory response. We found significant elevation in IL-1β, IL-6, and IL-8 in lung (Fig. 3A–C), of IL-1β and IL-8, but not IL-6, in intestine (Fig. 3D–F), and of IL-1β, IL-6, and IL-8 in brain (Fig. 3G–I). Newborns from IL-1β–treated dams administered 101.10 were protected, whereas Kineret had only a modest effect on some factors.

In utero exposure to IL-1β induces marked morphological alterations and malformations in lung, intestine, and brain of developing offspring

To determine whether the systemic inflammatory response triggered in newborns from IL-1β–treated dams was associated with abnormalities in organ development, as is observed in humans (3, 56), we studied litters from birth to PT15. Concordant with the unaffected neonatal weight observed between groups in viable pups (see Fig. 1H), growth from PT1 to PT13 was unaffected by treatments (Supplemental Fig. 2F). However, histological analysis of the lung, intestine, and brain revealed marked morphological alterations. Lungs of pups exposed to IL-1β displayed a grossly atypical lung parenchyma histology featuring disrupted alveolarization (Fig. 4A). Semiquantitative analysis of lung morphology revealed a 2-fold decrease in alveolar count induced by antenatal exposure to IL-1β (Fig. 4B) associated with a 2-fold increase in alveolar size (Fig. 4C), a significant decrease in septation count (Fig. 4D), and a 2-fold increase in parenchymal thickness (Fig. 4E). This phenotype was not observed in pups born from dams administered 101.10, whereas Kineret conveyed only partial improvement.

The intestine of pups from IL-1β–treated dams exhibited an abnormal shortening in villi (Fig. 5A, 5B) associated with an increased incidence of villous atrophy (Fig. 5C) in the jejunum–ileum. In the upstream intestine, this abnormality was associated with a marked loss in the quantity of colon-resident lymphoid follicles (Fig. 5D, 5E). The remaining follicles exhibited a significantly smaller size (Fig. 5F), suggesting compromised colon immunity. Treatment with 101.10 and Kineret both protected against jejunum–ileum and colon injury; however, Kineret was ineffective in normalizing the quantity of lymphoid follicles (see Fig. 5E).

In the brain, systemic perinatal inflammation impairs angiogenesis (57) to elicit major lifelong pathophysiological implications (58, 59). Perinatal brain injury is generally widespread throughout the brain, inferring an abnormality in vascularization (60). In pups exposed to IL-1β in utero, we found a significant microvascular degeneration in the cortex, cingulum, and hypothalamus (CA3 and dentate gyrus), but not in the striatum (Fig. 6A–G). This was associated with decreased brain weight that persisted to adulthood (Fig. 6H, 6I). Both 101.10 and Kineret prevented these injuries, with the exception that Kineret did not improve microvascular degeneration in the CA3 region of the hypothalamus.

Given the vascular impairment in the developing cortex of pups exposed in utero to IL-1β, and the loss in total brain mass, which is indicative of decay in cortical structure and function in humans (60), we conducted electrophysiological measurements of VEP to objectively assess cortical function in young adults. We found that young adults (PT30) exposed to IL-1β in the antenatal phase presented severe abnormalities in VEP performance, with a decreased amplitude and

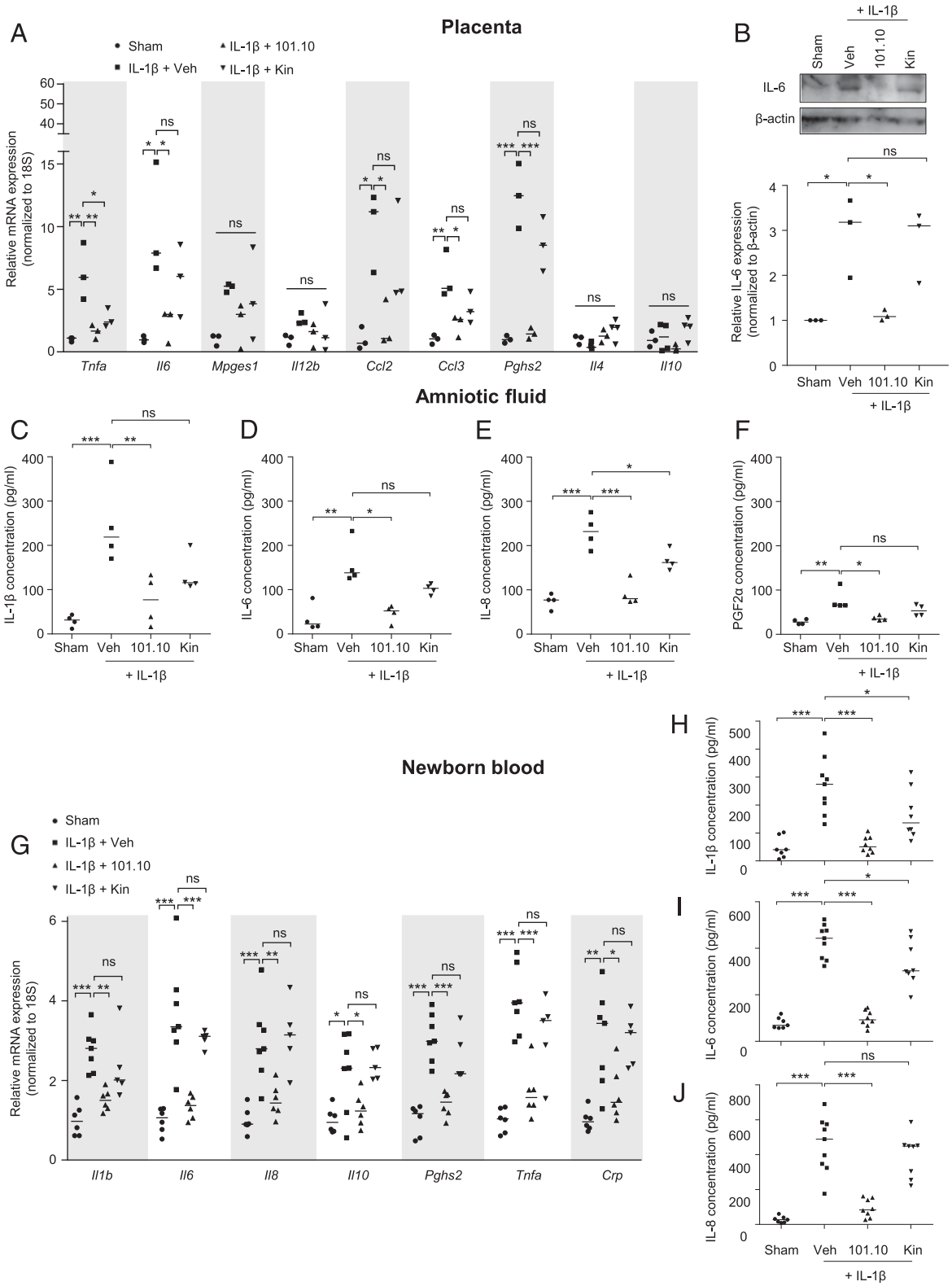

FIGURE 2. Inflammatory cytokines in the placenta, amniotic fluid, and neonatal blood are induced by antenatal exposure to IL-1β and corrected by 101.10. (**A** and **B**) Placentas were collected 24 h after uterine exposure to IL-1β to perform quantitative PCR (A) and immunoblots against IL-6 (B). PCR results are relative to 18S and plotted as fold change versus the control groups. Immunoblot quantification was normalized with β-actin and plotted as fold change versus sham. n = 3–4 dams per group. (**C–F**) Cytokine (IL-1, IL-6, and IL-8) and $PGF_{2\alpha}$ levels in amniotic fluids collected 24 h after IL-1β intrauterine exposure. n = 4 sacs per group. (**G**) Quantitative PCR performed on isolated WBCs from newborn pups. The blood of four to eight newborns per litter was pooled together to achieve sufficient mRNA levels. n = 5–7 dams per group. (**H–J**) Levels of IL-1, IL-6, and IL-8 in plasma samples from newborn pups. The blood of four to eight newborns per litter was pooled together to achieve sufficient mRNA levels. n = 7–9 dams per group. Individual values are presented with median. $^{*}p < 0.05$, $^{**}p < 0.01$, $^{***}p < 0.001$ by one-way ANOVA with a Dunnett postanalysis.

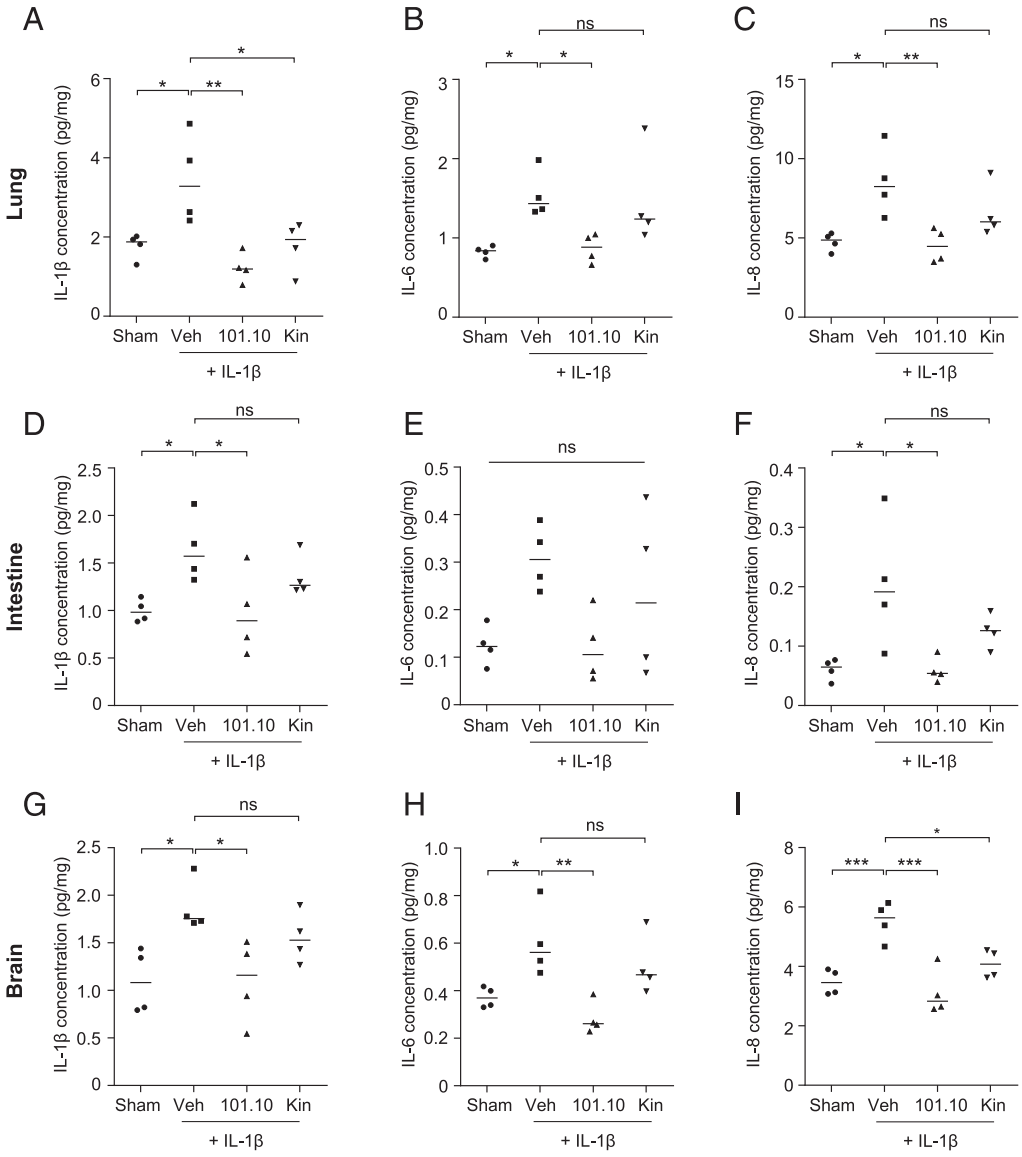

FIGURE 3. Inflammatory cytokines expression in the newborn lung, intestine, and brain is induced by antenatal exposure to IL-1β and corrected by 101.10. (**A–I**) Cytokine levels in lung (A–C), intestine (D–F), and brain (G–I) of newborns. $n = 4$ newborns per group. Individual values are presented with median. $*p < 0.05$, $**p < 0.01$, $***p < 0.001$ by one-way ANOVA with a Dunnett postanalysis.

delayed latency of key N2 and P2 components (Fig. 7A–C). These and other VEP anomalies were noted in 100% (six of six) of young adults exposed to IL-1β analyzed. Among the anomalies, absent VEP (characterized by unrecognizable P or N component) was observed in 50% of animals exposed to IL-1β (Fig. 7D; Supplemental Fig. 3A), suggesting a compromised cortical function that is concordant with observations in human infants with neurologic disorders (61). Antagonism of IL-1R by either 101.10 or Kineret prevented these outcomes.

101.10 prevents adverse obstetrical and perinatal outcomes triggered by LPS

Our previous data suggest that IL-1 is sufficient to trigger major adverse obstetric, perinatal, and developmental outcomes and identify 101.10 as an effective tool to prevent its action, whereas Kineret exhibits sporadic and attenuated efficacy (42, 62). We proceeded to investigate whether 101.10 exhibits effective therapeutic potential in a clinically relevant model triggered by bacterial products, an important upstream cause of uterine inflammation associated with poor neonatal outcomes (63); 0.5 μg of LPS, a dose shown previously to trigger robust IL-1 release (64), was administered (i.p.) at GD16.5 (Fig. 8A) and induced PTB (Fig. 8B), as amply documented by our group and others (42, 65). Accordingly, 101.10 decreased PTB induced by LPS with comparable efficacy as previously reported (42).

We found that 101.10 significantly improved LPS-induced survival at birth and at 1 wk of age (Fig. 8C–E). Viable pups did not display significant differences in weight at birth (Fig. 8F). Biochemical analysis of fetal–maternal tissue collected 4 h after LPS exposure revealed marked and consistent activation of major proinflammatory mRNA transcripts in the uterus (Fig. 9A), decidua (Fig. 9B), placenta (Fig. 9C), and fetal brain (Fig. 9D). The 101.10 significantly decreased activation of these genes, with the exception of uterine and placental *Il12b* ($p = 0.10$).

In a comprehensive analysis of offspring phenotype, growth trajectory from week 3 to week 20 (Supplemental Fig. 3B, 3C), as well as body morphometry of >20 tissues (Supplemental Table I) and serum adipocytokines assessed at week 20 of life to assess metabolic function (Supplemental Fig. 3D, 3E), were unaltered by treatment with 101.10 regardless of sex. Although 101.10 treatment caused a small reduction in body weight in male and female

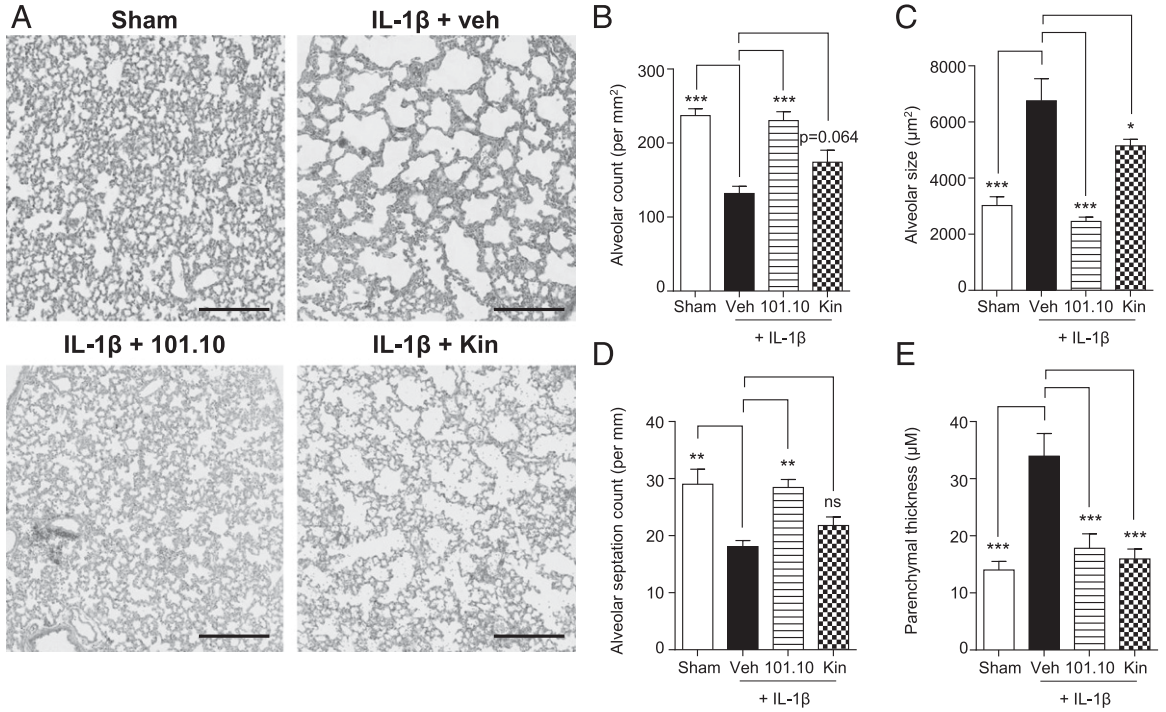

FIGURE 4. Lung injury in adolescent offspring is induced by antenatal exposure to IL-1β and corrected by 101.10. (**A**) Representative image of the lung parenchyma stained with H&E. Lungs were collected following in vivo formalin perfusion. Scale bars, 250 μm. (**B**–**E**) Measurement of alveolar count (B), alveolar size (C), alveolar septation count (D), and parenchymal thickness (E) performed on full tissue slides using Zen2 software. Data were collected on adolescent pups (PT15) from six to eight dams per group. Values are presented as mean ± SEM. ***$p < 0.001$ by one-way ANOVA with a Dunnett postanalysis.

pups at 4 wk of age after treatment, this was not seen when 101.10 was administered in combination with LPS. The only difference in adult offspring exposed to 101.10 plus LPS in utero was a 12% reduction in epididymis weight in males.

Discussion

Inflammation is an essential physiological mechanism employed by complex organisms to respond to infection and noninfectious insults, including oxidative stress, hypoxia/ischemia, and senescence. Inflammatory processes can become pathological depending on their location, timing, intensity, and chronicity. Overt inflammation, triggered by several stressors encountered by preterm infants, is a common upstream pathway observed in major perinatal diseases in the presence and absence of infection (10, 12, 13, 66, 67), including when excessive inflammation is triggered before birth (68). Accordingly, a causal relationship between inflammation and various neonatal diseases is firmly established (3, 14, 17–19).

Systemic inflammation of the fetus and newborn, referred to as FIRS, is clinically defined by elevated levels of IL-6 and other proinflammatory cytokines in fetal blood. FIRS is an independent risk factor of neonatal morbidity that affects multiple organs particularly the lung, intestine, and brain (3, 56, 66). In our study, we have shown that the inflammatory response to IL-1β in utero spreads from the uterine cavity to placenta and fetal membranes to induce a systemic fetal response characterized by a >4-fold increase in fetal plasma levels of IL-1β, IL-6, and IL-8 paralleled by leukocyte-mediated transcriptional induction of *Il1b*, *Il6*, and *IL8* and other proinflammatory genes. This fetal inflammatory response is known to result in morphological anomalies and injuries to lung, intestine, and brain (10–13).

Major organ injuries of the newborn associated with inflammation

Several tissues in the neonate are particularly prone to inflammatory damage that may begin before birth and be exacerbated by treatments and conditions to which the neonate is exposed. The immature lung of the premature infant is vulnerable to proinflammatory insults such as infection, hyperoxia, and mechanical stress and can therefore easily be injured by oxygen therapy, ventilation, or other insults in the first hours after birth. Pathological inflammation induces severe lung injuries in newborns, particularly those born preterm, characterized by loss in alveolar septation, reduced maturation of epithelial cells, parenchymal thickening, and diminished capillary density (27, 69, 70). During gestation, amniotic fluid is inhaled by the fetus and acts as an additional carrier of cytokines and other proinflammatory mediators to the fetal alveoli. Thus, antenatal exposure to intra-amniotic inflammation represents a strong and independent risk factor for the development of bronchopulmonary dysplasia (BPD) (4), an alveolar and vascular damage that results in pronounced disruption in alveolarization.

Inflammation is well recognized as a final common pathway to BPD wherein IL-1 is a critical contributor (17). Consistent with this, elevated cytokines (IL-1β, IL-6, and TNF-α) in the airway of premature newborns are associated with the onset of BPD (24, 71), and postnatal administration of IL-1 induces a BPD-like phenotype in mice (27). Pathological inflammation can begin before birth in the form of chorioamnionitis or related conditions, and stemming antenatal inflammation may improve the prospect for BPD (17). In the present study, we observed that lungs of pups born from IL-1β–treated dams displayed an increase in concentrations of various cytokines leading to severe morphological changes, consistent with features of BPD (70).

The gastrointestinal tract harbors the largest lymphoid tissue in the body consisting of resident lymphocytes grouped in follicles, but also of cells of the innate immune response such as macrophages and dendritic cells localized in the intestinal mucosa; these phagocytes present Ags to follicle-resident lymphocytes, coordinating immunologic defense mechanisms (72).

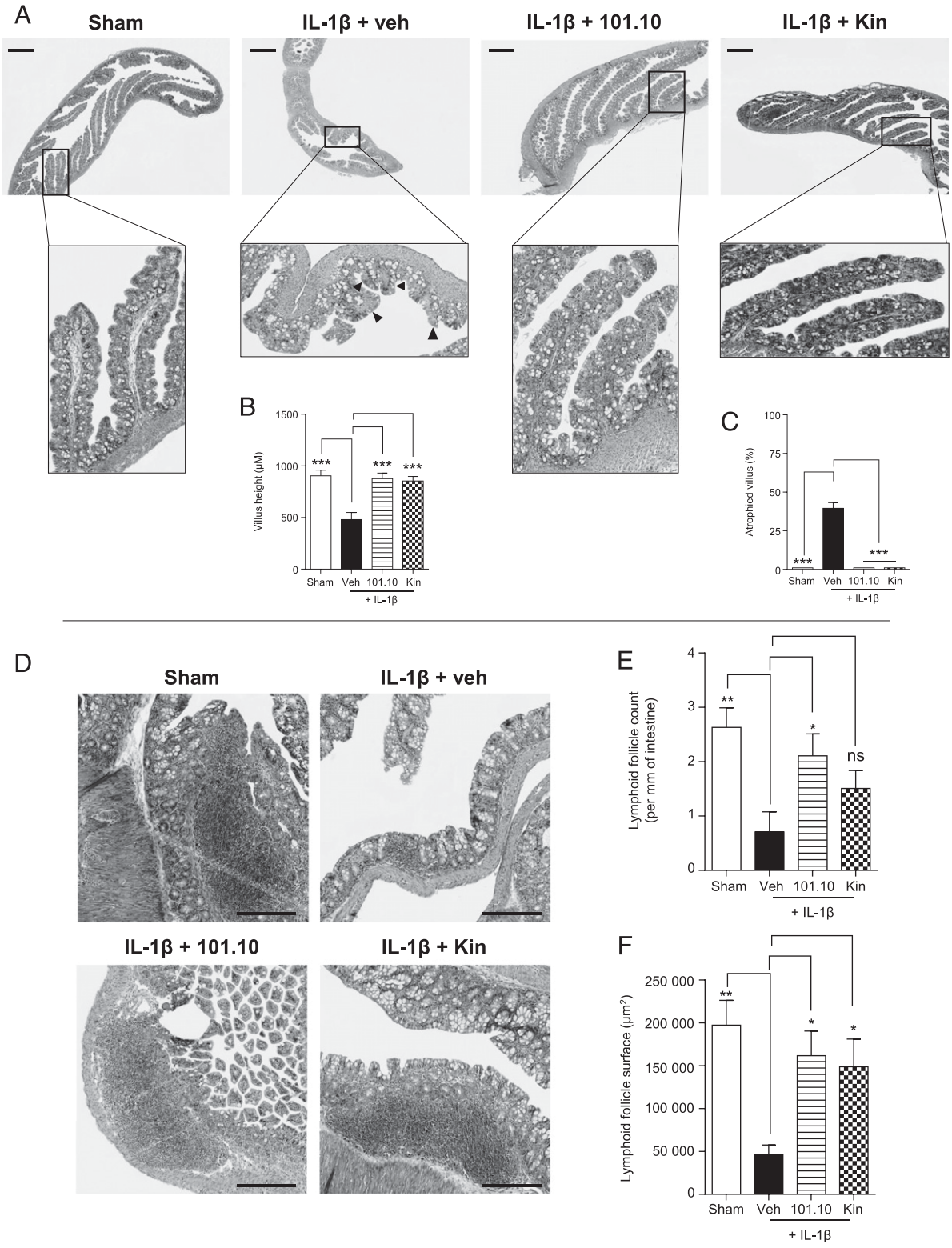

FIGURE 5. Morphological anomalies in intestine of adolescent offspring is induced by antenatal exposure to IL-1β and corrected by 101.10. (**A**) Representative images of intestinal villi integrity as assessed in hematoxylin/phloxine/safran-stained jejunum–ileum. Scale bars, 1000 μm. (**B** and **C**) Villi height was quantified using Zen2 software (B); atrophied villi were defined as villi measuring <400 μm and plotted as a percentage (C). (**D**) Representative images of hematoxylin/phloxine/safran-stained colon-resident lymphoid follicles. Scale bars, 250 μm. (**E** and **F**) Quantification of the number of lymphoid follicles (E) and their surface (F) was performed using Zen2 software. Data were collected on adolescent pups (PT15) from six to eight dams per group. Values are presented as means ± SEM. $*p < 0.05$, $**p < 0.01$, $***p < 0.001$ by one-way ANOVA with a Dunnett postanalysis.

Inflammation is a primary cause of necrotizing enterocolitis (NEC) (73). NEC is characterized by increased circulating and intestinal cytokines levels, including IL-1β, in neonates (21, 74) and a decreased expression of endogenous IL-1Ra is seen 2–3 wk prior to the onset of NEC (75). Correspondingly, targeting the inflammatory response in mice protects against experimental NEC (18).

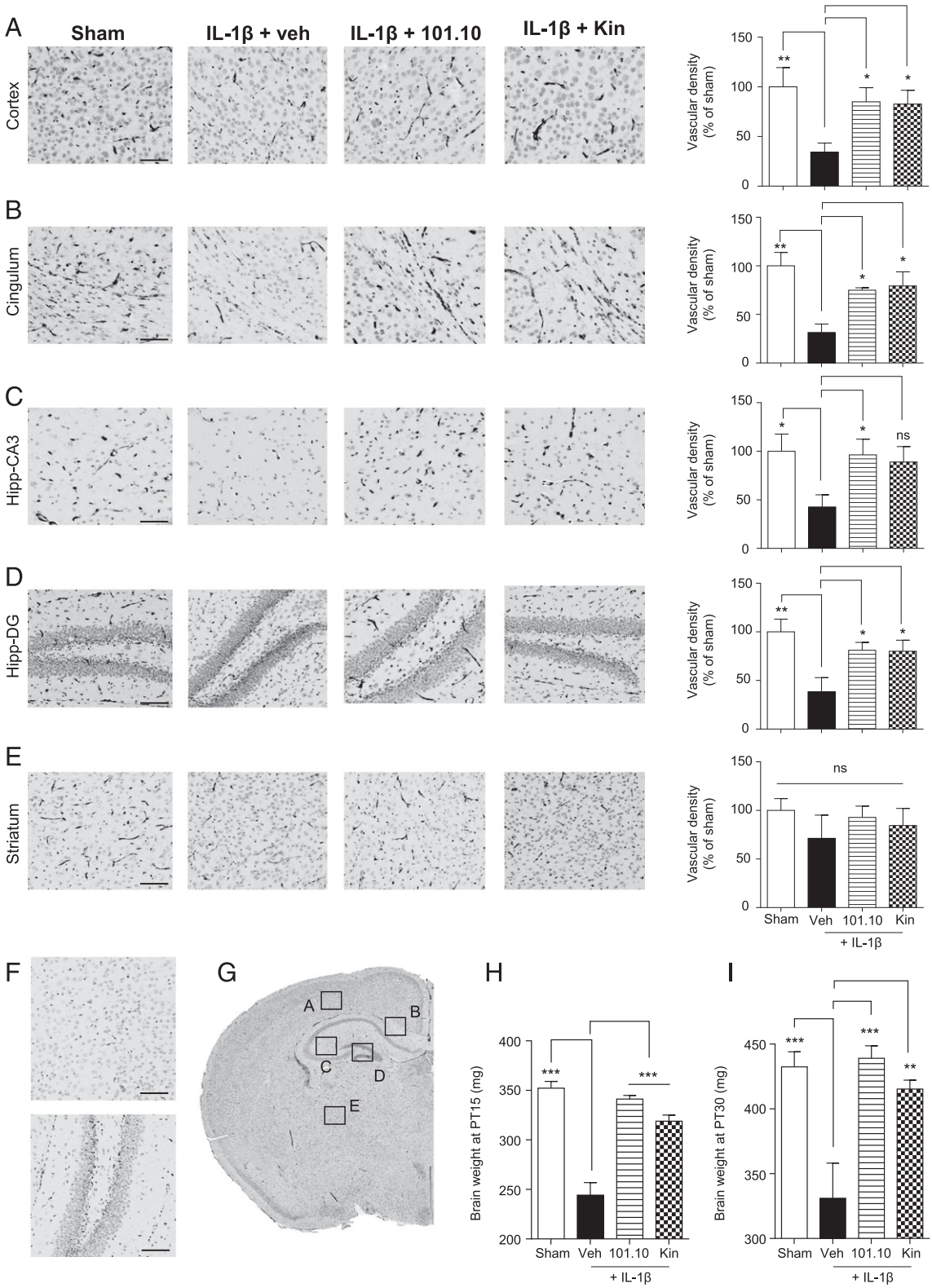

FIGURE 6. Microvascular degeneration in brain of adolescent offspring associated with cortical malfunction in adulthood is induced by antenatal exposure to IL-1β and corrected by 101.10. (**A**–**E**) Representative images and quantification of vessel density in cortex (A), cingulum (B), hypothalamus (C and D), and striatum (E) of adolescent pups. Immunostaining for lectin (vasculature, shown in brown) was separated from the purple hematoxylin using the color deconvolution function in ImageJ, and staining density was determined using ImageJ analysis software. Scale bars, 100 μM. (**F**) Negative control showing nonspecific staining. Scale bars, 100 μM. (**G**) Areas quantified are represented on the full cerebral right hemisphere micrograph. (**H** and **I**) Brain weight of adolescent pups (H) and young adults (I). Data were collected on adolescent pups (PT15) from six to eight dams per group and from young adults (PT30) from three to four dams per group (total of six to eight young adults per group). Values are presented as means ± SEM. $*p < 0.05$, $**p < 0.01$, $***p < 0.001$ by one-way ANOVA with a Dunnett postanalysis.

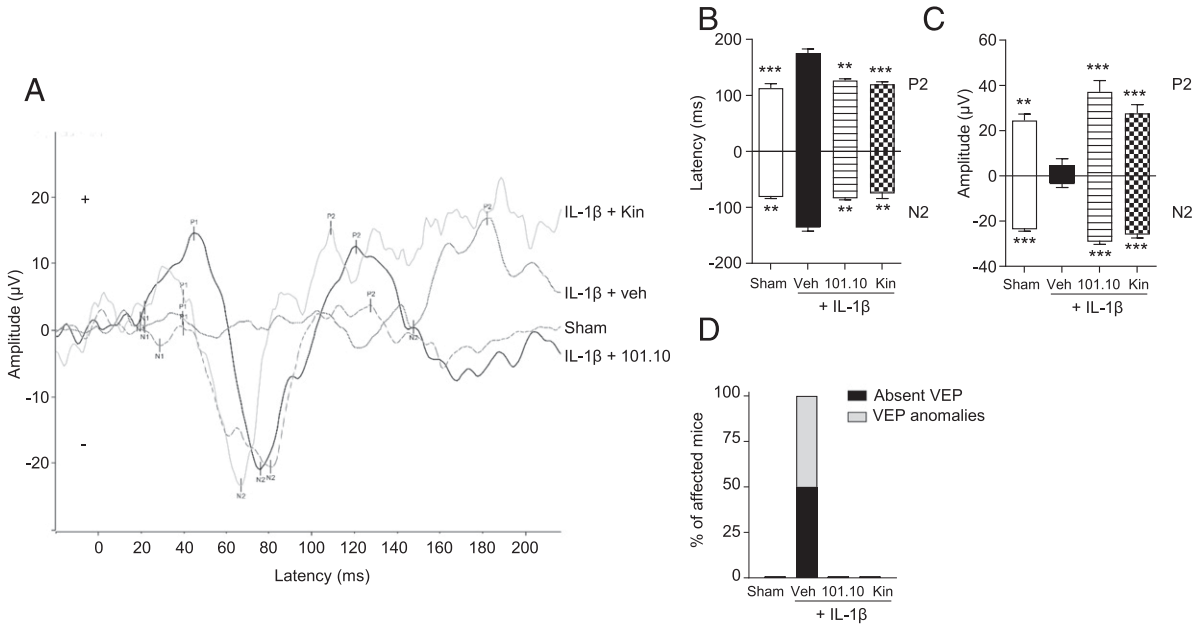

FIGURE 7. Cerebral functional impairment in adulthood is induced by antenatal exposure to IL-1β and corrected by 101.10. (**A**) Representative VEP measured on young adults (PT30) that were exposed during gestation to IL-1β with or without treatment with 101.10 or Kineret. (**B** and **C**) Latency (B) and amplitude (C) or the N2 and P2 components of the VEP. (**D**) Percentage of VEP anomalies and absent VEP in each group. VEP anomalies include significantly delayed latency or decreased amplitude of the P2 component, or absent VEP (see Supplemental Fig. 3A). Data were collected from six mice per group. Values are presented as mean ± SEM. $^{**}p < 0.01$, $^{***}p < 0.001$ by one-way ANOVA with a Dunnett postanalysis.

We found that exposure to IL-1β during gestation induced an increase in intestinal levels of IL-1β and IL-8 in newborns, leading to intestinal anomalies later in life. Specifically, villus integrity in the jejunum–ileum was severely compromised in young adolescent progeny exposed to IL-1, as reported in other models of neonatal intestinal injury (76, 77). Furthermore, a significant

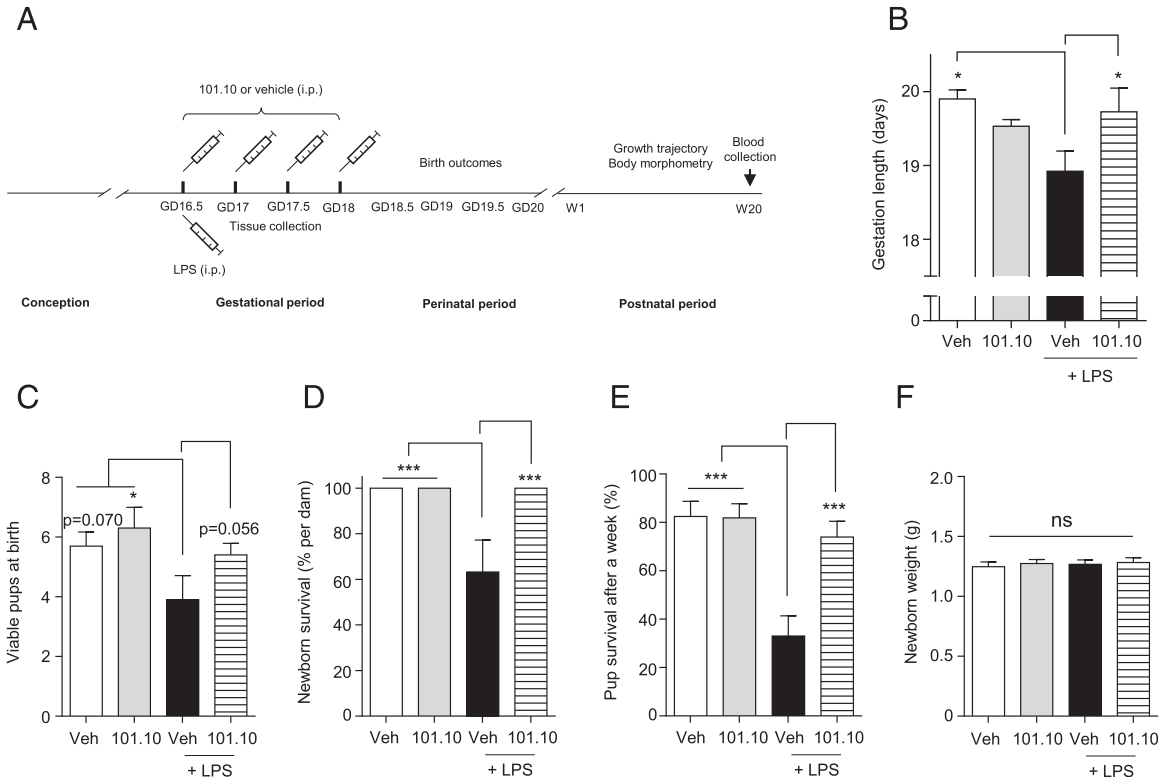

FIGURE 8. Therapeutic effect of 101.10 on gestational and perinatal outcomes following LPS treatment. (**A**) Pregnant females were given either LPS or vehicle i.p. on GD16.5, then 101.10 or vehicle at 12-h intervals on GD16.5, GD17.0, GD17.5, and GD18.0. (**B**–**D**) Gestation length (B), viable pup count (C), and pup survival rate as determined by counting breathing and nonbreathing pups at birth (D). (**E**) Pup survival rate at 1 wk (denominator represents viable pups at birth). (**F**) Pup weight at 12–24 h postbirth (denominator represents viable pups at birth). $n = 10$ dams per group. Values are presented as means ± SEM. $^{*}p < 0.05$, $^{***}p < 0.001$ by one-way ANOVA with a Dunnett postanalysis.

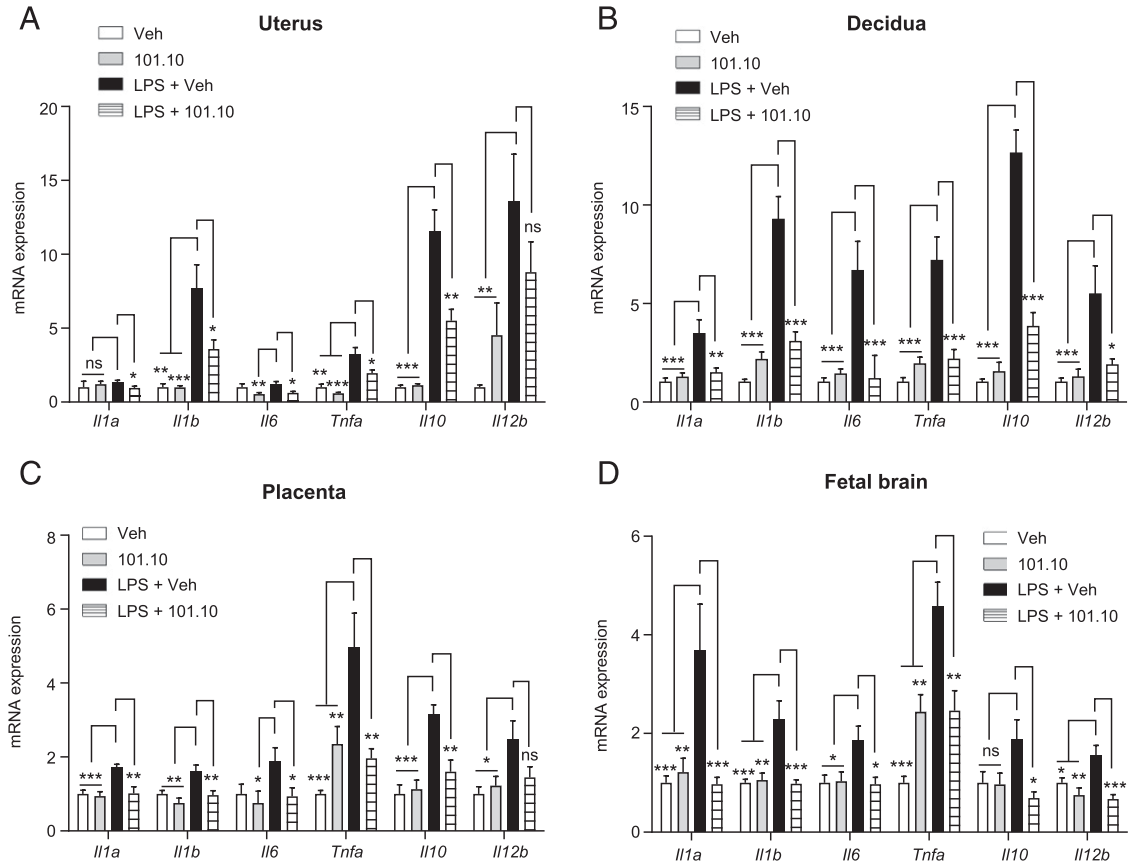

FIGURE 9. 101.10 protects against LPS-mediated induction of proinflammatory cytokines in gestational and fetal tissues. (**A**–**D**) Uterus (A), decidua (B), placenta (C), and fetal brain (D) were recovered from dams treated with LPS. Relative expression of *Il1a*, *Il1b*, *Il6*, *Tnf*, *Il10*, and *Il12b* mRNA transcripts were determined in each tissue by quantitative PCR normalized to *Actb*. Two implantation sites were collected per dam. $n = 12$ (6 dams per group). Values are presented as mean ± SEM. $*p < 0.05$, $**p < 0.01$, $***p < 0.001$ by one-way ANOVA with a Dunnett postanalysis.

decrease in the size and number of lymphoid follicles was observed, possibly predisposing to inadequate immune surveillance. Transcription factor NF-κB exerts a crucial role in maintaining intestinal immune surveillance (78) and, interestingly, NF-κB activity is preserved by 101.10, but abolished by Kineret (42), which may explain the inconsistent protective efficacy of Kineret in the colon.

Chorioamnionitis and antenatal exposure to inflammation causes major detriment to cerebral development (79). Numerous meta-analyses have linked chorioamnionitis to impairments of the newborn brain, including periventricular leukomalacia and cerebral palsy (80). Correspondingly, antenatal exposure of the fetus to inflammation is a strong and independent risk factor of cerebral palsy (5). Of all the cytokines implicated, IL-1 stands out, as preclinical and clinical evidence suggests it directly induces neurotoxicity (81), whereas its blockade using pharmacological or genetic approaches exerts neuroprotective effects in animal models (19, 62). A systematic review of 47 studies with a positive correlation between cytokine and neonatal infection or neurologic insults concurs that levels of IL-1β in cord or neonatal blood are augmented in 100% of patients with neurologic insults (82).

Fetal and neonatal inflammation is widespread throughout the neural vascular network (33, 83), resulting in generalized microvascular degeneration, which in turn causes diffuse injury to the brain resulting in globally reduced brain mass, volume, and function, as observed in similar rodent studies (33, 84) as well as in extreme premature infants (60).

VEP provides an objective assessment of brain function and is regularly used in infants to identify brain pathology (85). In this context, a study by Kato et al. (61) reported VEP anomalies (including absent VEP) in all infants suffering from periventricular leukomalacia. In line with this, pups exposed to IL-1β presented VEP anomalies, and absent VEP was observed in 50% of cases. In utero antagonism of IL-1R abrogated IL-1–induced cerebral inflammation at birth and its consequences for the vascular network, brain weight, and VEP, demonstrating an efficacy comparable to that of neuroprotective therapies delivered to the neonate (62, 86). A similar efficacy of 101.10 was observed in relevant LPS-treated animals (see Fig. 9).

Pathophysiological contribution to neonatal diseases: inflammation versus prematurity

It is not clear whether the consequences of intrauterine inflammation in infants eventuate due to shorter gestation and immaturity at birth, or directly due to detrimental effects of inflammation on tissues (3, 86). Compelling clinical evidence points to antenatal inflammation in tissue injury independent of gestation length (3–6, 56, 66, 87). This body of evidence is complemented with preclinical data clearly demonstrating that: 1) induction of PTB in mice using intrauterine infusion of proinflammatory LPS at GD15 induces an elevation in cerebral cytokine levels and neurologic injury to the fetus, whereas none of these features is observed when PTB is induced using a noninflammatory model of progesterone inhibition (88); 2) administration of LPS to pregnant mice at GD15 and GD18 induces comparable acute injury to fetal brain, despite that pregnant mice treated at GD15 deliver prematurely, whereas those treated at GD18 deliver at term (89); 3) intrauterine administration of LPS in pregnant mice at term induces inflammation in the fetal brain and causes neurotoxicity

(90) consistent with clinical evidence that chorioamnionitis at term can impair neurobehavioral outcome in infants (91–94); and 4) administration of Kineret to pregnant mice treated with LPS improves neurologic outcomes without preventing PTB (62), as reaffirmed in the present study. Overall, this suggests that both preterm labor and inflammation need to be tackled by effective and targeted therapeutics to improve gestation outcome. This study uncovers a pivotal contribution of IL-1 in this process, and it shows that targeting IL-1 is effective in preventing fetal inflammatory injury in an infection model.

Contrast in efficacy between 101.10 and Kineret

Although both 101.10 and Kineret elicit improved outcomes for tissue integrity of progeny after IL-1 exposure, 101.10 is more consistently effective than Kineret in other aspects, particularly in inhibiting in utero inflammation, preventing PTB, and improving neonatal mortality. The inefficacy of Kineret to block in utero inflammation and PTB is related to dose, suggesting that the uterine inflammation responsible for preterm labor is more pronounced and difficult to tackle than the placental response leading to neonatal inflammatory injury. This is supported by the fact that Kineret (standard dose of 4 mg/kg per 12 h) elicits a modest (albeit not statistically significant) inhibition of essentially all inflammatory mediators, which leads to lower levels of cytokines in the fetal amniotic fluid as well as in fetal tissues per se. Correspondingly, these observations on Kineret in fetal–placental inflammation also apply to LPS-induced PTB (62). Accordingly, lower (standard) doses of Kineret are able to reduce placental inflammation sufficiently to convey protection to the fetus (62, 86); alternatively, prevention of PTB needs much higher doses of Kineret to inhibit inflammatory factors to a greater degree in the uteroplacental compartment. This disparity in potency may be due to pharmacological considerations, including: 1) competitive antagonists rely on high concentrations at the site of action to establish a favorable antagonist/agonist ratio, whereas noncompetitive antagonists bind to a site remote from the natural ligand binding site and their effects are for the most part independent of agonist concentrations (95); and 2) small molecules such as 101.10 (0.85 kDa) have increased access and distribution to tissue. However, neither 101.10 (as shown herein) nor Kineret (96) crosses the placenta in significant amounts even under inflammatory conditions, suggesting that their therapeutic effects on pups are mediated indirectly through actions in the maternal gestational tissues that spread inflammation into the fetal–placental and tissue compartments.

In conclusion, in the present study we report harmful effects of antenatal exposure to IL-1 on the development of progeny from intrauterine life to adulthood, and we demonstrate that suppression of IL-1 signaling using a novel peptide inhibitor of the IL-1 receptor is efficacious in rescuing pups from injury in an LPS-induced model of fetal inflammatory insult. This study has implications for the development of therapeutic molecules for pregnancy disorders wherein IL-1 plays a pathophysiological role such as chorioamnionitis, which affects a significant proportion of PTB and is associated with adverse neonatal outcomes independently of the duration of gestation. Our study substantiates the increasing evidence suggesting that it is insufficient simply to tackle uterine contractions in preterm labor to ultimately improve neonatal outcome. Suppressing the harmful effects of an excessive antenatal exposure to IL-1 using 101.10 during pregnancy appears to be a safe, potent, and effective therapeutic modality to protect the fetus exposed to intrauterine inflammation. As a small molecule able to access the placental tissue, 101.10 may have therapeutic advantages over the currently available drug Kineret.

Acknowledgments

We graciously thank Isabelle Lahaie and Irène Londono for technical assistance provided and Dr. Marie-Sylvie Roy and Dr. Jacqueline Orquin for help provided in analyzing murine VEP and for reviewing the manuscript.

Disclosures

S.C., C.Q., and W.D.L. hold a patent on composition of matter for the use of 101.10 (IL-1 receptor antagonists, compositions, and methods of treatment, United States patent no. USPTO8618054, May 5, 2005). The remaining authors have no financial conflicts of interest.

References

1. Blencowe, H., S. Cousens, D. Chou, M. Oestergaard, L. Say, A. B. Moller, M. Kinney, and J. Lawn, Born Too Soon Preterm Birth Action Group. 2013. Born too soon: the global epidemiology of 15 million preterm births. *Reprod. Health* 10(Suppl. 1): S2.
2. Romero, R., J. Miranda, T. Chaiworapongsa, S. J. Korzeniewski, P. Chaemsaithong, F. Gotsch, Z. Dong, A. I. Ahmed, B. H. Yoon, S. S. Hassan, et al. 2014. Prevalence and clinical significance of sterile intra-amniotic inflammation in patients with preterm labor and intact membranes. *Am. J. Reprod. Immunol.* 72: 458–474.
3. Gotsch, F., R. Romero, J. P. Kusanovic, S. Mazaki-Tovi, B. L. Pineles, O. Erez, J. Espinoza, and S. S. Hassan. 2007. The fetal inflammatory response syndrome. *Clin. Obstet. Gynecol.* 50: 652–683.
4. Yoon, B. H., R. Romero, K. S. Kim, J. S. Park, S. H. Ki, B. I. Kim, and J. K. Jun. 1999. A systemic fetal inflammatory response and the development of bronchopulmonary dysplasia. *Am. J. Obstet. Gynecol.* 181: 773–779.
5. Yoon, B. H., R. Romero, J. S. Park, C. J. Kim, S. H. Kim, J. H. Choi, and T. R. Han. 2000. Fetal exposure to an intra-amniotic inflammation and the development of cerebral palsy at the age of three years. *Am. J. Obstet. Gynecol.* 182: 675–681.
6. Bracci, R., and G. Buonocore. 2003. Chorioamnionitis: a risk factor for fetal and neonatal morbidity. *Biol. Neonate* 83: 85–96.
7. Witt, A., A. Berger, C. J. Gruber, L. Petricevic, P. Apfalter, and P. Husslein. 2005. IL-8 concentrations in maternal serum, amniotic fluid and cord blood in relation to different pathogens within the amniotic cavity. *J. Perinat. Med.* 33: 22–26.
8. McAdams, R. M., and S. E. Juul. 2012. The role of cytokines and inflammatory cells in perinatal brain injury. *Neurol. Res. Int.* 2012: 561494.
9. Hanzl, M. 2009. Relationship between cytokine IL 6 levels and early-onset neonatal morbidity. *Neuroendocrinol. Lett.* 30: 535–539.
10. Iliodromiti, Z., D. Zygouris, S. Sifakis, K. I. Pappa, P. Tsikouras, N. Salakos, A. Daniilidis, C. Siristatidis, and N. Vrachnis. 2013. Acute lung injury in preterm fetuses and neonates: mechanisms and molecular pathways. *J. Matern. Fetal Neonatal Med.* 26: 1696–1704.
11. American College of Obstetricians and Gynecologists. 2013. ACOG committee opinion no. 561: nonmedically indicated early-term deliveries. *Obstet. Gynecol.* 121: 911–915.
12. Rees, S., and T. Inder. 2005. Fetal and neonatal origins of altered brain development. *Early Hum. Dev.* 81: 753–761.
13. Claud, E. C. 2009. Neonatal necrotizing enterocolitis -inflammation and intestinal immaturity. *Antiinflamm. Antiallergy Agents Med. Chem.* 8: 248–259.
14. Toso, L., S. Poggi, J. Park, H. Einat, R. Roberson, V. Dunlap, J. Woodard, D. Abebe, and C. Y. Spong. 2005. Inflammatory-mediated model of cerebral palsy with developmental sequelae. *Am. J. Obstet. Gynecol.* 193: 933–941.
15. Karatepe, H. O., H. Kilincaslan, M. Berber, A. Ozen, H. E. Saricoban, D. Ustek, A. S. Kemik, M. Adas, and F. Bakar. 2014. The effect of vascular endothelial growth factor overexpression in experimental necrotizing enterocolitis. *Pediatr. Surg. Int.* 30: 327–332.
16. Gortner, L., D. Monz, C. Mildau, J. Shen, M. Kasoha, M. W. Laschke, T. Roolfs, A. Schmiedl, C. Meier, and E. Tutdibi. 2013. Bronchopulmonary dysplasia in a double-hit mouse model induced by intrauterine hypoxia and postnatal hyperoxia: closer to clinical features? *Ann. Anat.* 195: 351–358.
17. Nold, M. F., N. E. Mangan, I. Rudloff, S. X. Cho, N. Shariatian, T. D. Samarasinghe, E. M. Skuza, J. Pedersen, A. Veldman, P. J. Berger, and C. A. Nold-Petry. 2013. Interleukin-1 receptor antagonist prevents murine bronchopulmonary dysplasia induced by perinatal inflammation and hyperoxia. *Proc. Natl. Acad. Sci. USA* 110: 14384–14389.
18. Yurttutan, S., R. Ozdemir, F. E. Canpolat, M. Y. Oncel, H. G. Unverdi, B. Uysal, Ö. Erdeve, and U. Dilmen. 2014. Beneficial effects of Etanercept on experimental necrotizing enterocolitis. *Pediatr. Surg. Int.* 30: 71–77.
19. Girard, S., H. Sébire, M. E. Brochu, S. Briota, P. Sarret, and G. Sébire. 2012. Postnatal administration of IL-1Ra exerts neuroprotective effects following perinatal inflammation and/or hypoxic-ischemic injuries. *Brain Behav. Immun.* 26: 1331–1339.
20. Romero, R., S. K. Dey, and S. J. Fisher. 2014. Preterm labor: one syndrome, many causes. *Science* 345: 760–765.
21. Edelson, M. B., C. E. Bagwell, and H. J. Rozycki. 1999. Circulating pro- and counterinflammatory cytokine levels and severity in necrotizing enterocolitis. *Pediatrics* 103: 766–771.

22. Kakkera, D. K., M. M. Siddiq, and L. A. Parton. 2005. Interleukin-1 balance in the lungs of preterm infants who develop bronchopulmonary dysplasia. *Biol. Neonate* 87: 82–90.
23. Basu, S., P. Agarwal, S. Anupurba, R. Shukla, and A. Kumar. 2015. Elevated plasma and cerebrospinal fluid interleukin-1β and tumor necrosis factor-alpha concentration and combined outcome of death or abnormal neuroimaging in preterm neonates with early-onset clinical sepsis. *J. Perinatol.* 35: 855–861.
24. Cayabyab, R. G., C. A. Jones, K. Y. Kwong, C. Hendershott, C. Lecart, P. Minoo, and R. Ramanathan. 2003. Interleukin-1β in the bronchoalveolar lavage fluid of premature neonates: a marker for maternal chorioamnionitis and predictor of adverse neonatal outcome. *J. Matern. Fetal Neonatal Med.* 14: 205–211.
25. Fan, L. W., L. T. Tien, B. Zheng, Y. Pang, P. G. Rhodes, and Z. Cai. 2010. Interleukin-1β-induced brain injury and neurobehavioral dysfunctions in juvenile rats can be attenuated by α-phenyl-*n*-*tert*-butyl-nitrone. *Neuroscience* 168: 240–252.
26. Nikiforou, M., M. W. Kemp, R. H. van Gorp, M. Saito, J. P. Newnham, N. L. Reynaert, L. E. Janssen, A. H. Jobe, S. G. Kallapur, B. W. Kramer, and T. G. Wolfs. 2016. Selective IL-1α exposure to the fetal gut, lung, and chorioamnion/skin causes intestinal inflammatory and developmental changes in fetal sheep. *Lab. Invest.* 96: 69–80.
27. Bry, K., J. A. Whitsett, and U. Lappalainen. 2007. IL-1β disrupts postnatal lung morphogenesis in the mouse. *Am. J. Respir. Cell Mol. Biol.* 36: 32–42.
28. Savard, A., M. E. Brochu, M. Chevin, C. Guiraut, D. Grbic, and G. Sébire. 2015. Neuronal self-injury mediated by IL-1β and MMP-9 in a cerebral palsy model of severe neonatal encephalopathy induced by immune activation plus hypoxia-ischemia. *J. Neuroinflammation* 12: 111.
29. Savard, A., K. Lavoie, M. E. Brochu, D. Grbic, M. Lepage, D. Gris, and G. Sebire. 2013. Involvement of neuronal IL-1β in acquired brain lesions in a rat model of neonatal encephalopathy. *J. Neuroinflammation* 10: 110.
30. Kallapur, S. G., I. Nitsos, T. J. Moss, G. R. Polglase, J. J. Pillow, F. C. Cheah, B. W. Kramer, J. P. Newnham, M. Ikegami, and A. H. Jobe. 2009. IL-1 mediates pulmonary and systemic inflammatory responses to chorioamnionitis induced by lipopolysaccharide. *Am. J. Respir. Crit. Care Med.* 179: 955–961.
31. Hara, H., R. M. Friedlander, V. Gagliardini, C. Ayata, K. Fink, Z. Huang, M. Shimizu-Sasamata, J. Yuan, and M. A. Moskowitz. 1997. Inhibition of interleukin 1β converting enzyme family proteases reduces ischemic and excitotoxic neuronal damage. *Proc. Natl. Acad. Sci. USA* 94: 2007–2012.
32. Zhou, T. E., J. C. Rivera, V. K. Bhosle, I. Lahaie, Z. Shao, H. Tahiri, T. Zhu, A. Polosa, A. Dorfman, A. Beaudry-Richard, et al. 2016. Choroidal involution is associated with a progressive degeneration of the outer retinal function in a model of retinopathy of prematurity: early role for IL-1β. *Am. J. Pathol.* 186: 3100–3116.
33. Rivera, J. C., N. Sitaras, B. Noueihed, D. Hamel, A. Madaan, T. Zhou, J. C. Honoré, C. Quiniou, J. S. Joyal, P. Hardy, et al. 2013. Microglia and interleukin-1β in ischemic retinopathy elicit microvascular degeneration through neuronal semaphorin-3A. *Arterioscler. Thromb. Vasc. Biol.* 33: 1881–1891.
34. Zhang, K., H. Xu, L. Cao, K. Li, and Q. Huang. 2013. Interleukin-1β inhibits the differentiation of hippocampal neural precursor cells into serotonergic neurons. *Brain Res.* 1490: 193–201.
35. Medel-Matus, J. S., D. M. Álvarez-Croda, J. Martínez-Quiroz, L. Beltrán-Parrazal, C. Morgado-Valle, and M. L. López-Meraz. 2014. IL-1β increases necrotic neuronal cell death in the developing rat hippocampus after status epilepticus by activating type I IL-1 receptor (IL-1RI). *Int. J. Dev. Neurosci.* 38: 232–240.
36. Romero, R., P. Chaemsaithong, N. Docheva, S. J. Korzeniewski, A. L. Tarca, G. Bhatti, Z. Xu, J. P. Kusanovic, Z. Dong, N. Chaiyasit, et al. 2016. Clinical chorioamnionitis at term IV: the maternal plasma cytokine profile. *J. Perinat. Med.* 44: 77–98.
37. Yoon, B. H., J. K. Jun, R. Romero, K. H. Park, R. Gomez, J. H. Choi, and I. O. Kim. 1997. Amniotic fluid inflammatory cytokines (interleukin-6, interleukin-1β, and tumor necrosis factor-alpha), neonatal brain white matter lesions, and cerebral palsy. *Am. J. Obstet. Gynecol.* 177: 19–26.
38. Burd, I., B. Balakrishnan, and S. Kannan. 2012. Models of fetal brain injury, intrauterine inflammation, and preterm birth. *Am. J. Reprod. Immunol.* 67: 287–294.
39. Romero, R., D. T. Brody, E. Oyarzun, M. Mazor, Y. K. Wu, J. C. Hobbins, and S. K. Durum. 1989. Infection and labor. III. Interleukin-1: a signal for the onset of parturition. *Am. J. Obstet. Gynecol.* 160: 1117–1123.
40. Romero, R., M. Mazor, and B. Tartakovsky. 1991. Systemic administration of interleukin-1 induces preterm parturition in mice. *Am. J. Obstet. Gynecol.* 165: 969–971.
41. Sadowsky, D. W., K. M. Adams, M. G. Gravett, S. S. Witkin, and M. J. Novy. 2006. Preterm labor is induced by intraamniotic infusions of interleukin-1β and tumor necrosis factor-α but not by interleukin-6 or interleukin-8 in a nonhuman primate model. *Am. J. Obstet. Gynecol.* 195: 1578–1589.
42. Nadeau-Vallée, M., C. Quiniou, J. Palacios, X. Hou, A. Erfani, A. Madaan, M. Sanchez, K. Leimert, A. Boudreault, F. Duhamel, et al. 2015. Novel noncompetitive IL-1 receptor-biased ligand prevents infection- and inflammation-induced preterm birth. *J. Immunol.* 195: 3402–3415.
43. Nadeau-Vallée, M., D. Obari, C. Quiniou, W. D. Lubell, D. M. Olson, S. Girard, and S. Chemtob. 2016. A critical role of interleukin-1 in preterm labor. *Cytokine Growth Factor Rev.* 28: 37–51.
44. Quiniou, C., P. Sapieha, I. Lahaie, X. Hou, S. Brault, M. Beauchamp, M. Leduc, L. Rihakova, J. S. Joyal, S. Nadeau, et al. 2008. Development of a novel noncompetitive antagonist of IL-1 receptor. *J. Immunol.* 180: 6977–6987.
45. Allport, V. C., D. M. Slater, R. Newton, and P. R. Bennett. 2000. NF-κB and AP-1 are required for cyclo-oxygenase 2 gene expression in amnion epithelial cell line (WISH). *Mol. Hum. Reprod.* 6: 561–565.
46. Khanjani, S., V. Terzidou, M. R. Johnson, and P. R. Bennett. 2012. NFκB and AP-1 drive human myometrial IL8 expression. *Mediators Inflamm.* 2012: 504952.
47. Deng, X., M. Xu, C. Yuan, L. Yin, X. Chen, X. Zhou, G. Li, Y. Fu, C. A. Feghali-Bostwick, and L. Pang. 2013. Transcriptional regulation of increased CCL2 expression in pulmonary fibrosis involves nuclear factor-κB and activator protein-1. *Int. J. Biochem. Cell Biol.* 45: 1366–1376.
48. MacIntyre, D. A., Y. S. Lee, R. Migale, B. R. Herbert, S. N. Waddington, D. Peebles, H. Hagberg, M. R. Johnson, and P. R. Bennett. 2014. Activator protein 1 is a key terminal mediator of inflammation-induced preterm labor in mice. *FASEB J.* 28: 2358–2368.
49. Jamieson, A. G., N. Boutard, K. Beauregard, M. S. Bodas, H. Ong, C. Quiniou, S. Chemtob, and W. D. Lubell. 2009. Positional scanning for peptide secondary structure by systematic solid-phase synthesis of amino lactam peptides. *J. Am. Chem. Soc.* 131: 7917–7927.
50. Boutard, N., S. Turcotte, K. Beauregard, C. Quiniou, S. Chemtob, and W. D. Lubell. 2011. Examination of the active secondary structure of the peptide 101.10, an allosteric modulator of the interleukin-1 receptor, by positional scanning using β-amino γ-lactams. *J. Pept. Sci.* 17: 288–296.
51. Lavoie, J. C., T. Rouleau, A. Tsopmo, J. Friel, and P. Chessex. 2008. Influence of lung oxidant and antioxidant status on alveolarization: role of light-exposed total parenteral nutrition. *Free Radic. Biol. Med.* 45: 572–577.
52. Nadeau-Vallée, M., A. Boudreault, K. Leimert, X. Hou, D. Obari, A. Madaan, R. Rouget, T. Zhu, L. Belarbi, M. E. Brien, et al. 2016. Uterotonic neuromedin U receptor 2 and its ligands are upregulated by inflammation in mice and humans, and elicit preterm birth. *Biol. Reprod.* 95: 72.
53. Girard, S., G. Sébire, and H. Kadhim. 2010. Proinflammatory orientation of the interleukin 1 system and downstream induction of matrix metalloproteinase 9 in the pathophysiology of human perinatal white matter damage. *J. Neuropathol. Exp. Neurol.* 69: 1116–1129.
54. Yoshimura, K., and E. Hirsch. 2005. Effect of stimulation and antagonism of interleukin-1 signaling on preterm delivery in mice. *J. Soc. Gynecol. Investig.* 12: 533–538.
55. Combs, C. A., M. Gravett, T. J. Garite, D. E. Hickok, J. Lapidus, R. Porreco, J. Rael, T. Grove, T. K. Morgan, W. Clewell, et al. 2014. Amniotic fluid infection, inflammation, and colonization in preterm labor with intact membranes. *Am. J. Obstet. Gynecol.* 210: 125.e1–125.e15.
56. Gomez, R., R. Romero, F. Ghezzi, B. H. Yoon, M. Mazor, and S. M. Berry. 1998. The fetal inflammatory response syndrome. *Am. J. Obstet. Gynecol.* 179: 194–202.
57. Hong, H. K., H. J. Lee, J. H. Ko, J. H. Park, J. Y. Park, C. W. Choi, C. H. Yoon, S. J. Ahn, K. H. Park, S. J. Woo, and J. Y. Oh. 2014. Neonatal systemic inflammation in rats alters retinal vessel development and simulates pathologic features of retinopathy of prematurity. *J. Neuroinflammation* 11: 87.
58. Kalaria, R. N. 2010. Vascular basis for brain degeneration: faltering controls and risk factors for dementia. *Nutr. Rev.* 68(Suppl. 2): S74–S87.
59. Girard, S., H. Kadhim, N. Beaudet, P. Sarret, and G. Sébire. 2009. Developmental motor deficits induced by combined fetal exposure to lipopolysaccharide and early neonatal hypoxia/ischemia: a novel animal model for cerebral palsy in very premature infants. *Neuroscience* 158: 673–682.
60. Abernethy, L. J., R. W. Cooke, and L. Foulder-Hughes. 2004. Caudate and hippocampal volumes, intelligence, and motor impairment in 7-year-old children who were born preterm. *Pediatr. Res.* 55: 884–893.
61. Kato, T., A. Okumura, F. Hayakawa, K. Kuno, and K. Watanabe. 2005. The evolutionary change of flash visual evoked potentials in preterm infants with periventricular leukomalacia. *Clin. Neurophysiol.* 116: 690–695.
62. Leitner, K., M. Al Shammary, M. McLane, M. V. Johnston, M. A. Elovitz, and I. Burd. 2014. IL-1 receptor blockade prevents fetal cortical brain injury but not preterm birth in a mouse model of inflammation-induced preterm birth and perinatal brain injury. *Am. J. Reprod. Immunol.* 71: 418–426.
63. Cornette, L. 2005. Perinatal inflammation and infection. *Minerva Ginecol.* 57: 411–421.
64. Girard, S., H. Kadhim, A. Larouche, M. Roy, F. Gobeil, and G. Sébire. 2008. Pro-inflammatory disequilibrium of the IL-1β/IL-1ra ratio in an experimental model of perinatal brain damages induced by lipopolysaccharide and hypoxia–ischemia. *Cytokine* 43: 54–62.
65. Huang, L., A. M. Krieg, N. Eller, and D. E. Scott. 1999. Induction and regulation of Th1-inducing cytokines by bacterial DNA, lipopolysaccharide, and heat-inactivated bacteria. *Infect. Immun.* 67: 6257–6263.
66. Hofer, N, R Kothari, N Morris, W Muller, and B Resch. 2013. The fetal inflammatory response syndrome is a risk factor for morbidity in preterm neonates. *Am. J. Obstet. Gynecol.* 209: 542.e1–542.e11.
67. Nadeau-Vallée, M., D. Obari, J. Palacios, M. E. Brien, C. Duval, S. Chemtob, and S. Girard. 2016. Sterile inflammation and pregnancy complications: a review. *Reproduction* 152: R277–R292.
68. Lau, J., F. Magee, Z. Qiu, J. Houbé, P. Von Dadelszen, and S. K. Lee. 2005. Chorioamnionitis with a fetal inflammatory response is associated with higher neonatal mortality, morbidity, and resource use than chorioamnionitis displaying a maternal inflammatory response only. *Am. J. Obstet. Gynecol.* 193: 708–713.
69. Bose, C. L., C. E. Dammann, and M. M. Laughon. 2008. Bronchopulmonary dysplasia and inflammatory biomarkers in the premature neonate. *Arch. Dis. Child. Fetal Neonatal Ed.* 93: F455–F461.
70. Coalson, J. J. 2003. Pathology of new bronchopulmonary dysplasia. *Semin. Neonatol.* 8: 73–81.
71. Köksal, N., B. Kayik, M. Çetinkaya, H. Özkan, F. Budak, Ş. Kiliç, Y. Canitez, and B. Oral. 2012. Value of serum and bronchoalveolar fluid lavage pro- and anti-inflammatory cytokine levels for predicting bronchopulmonary dysplasia in premature infants. *Eur. Cytokine Netw.* 23: 29–35.

72. Mowat, A. M., and J. L. Viney. 1997. The anatomical basis of intestinal immunity. *Immunol. Rev.* 156: 145–166.
73. Cho, S. X., P. J. Berger, C. A. Nold-Petry, and M. F. Nold. 2016. The immunological landscape in necrotising enterocolitis. *Expert Rev. Mol. Med.* 18: e12.
74. Bhatia, A. M., B. J. Stoll, M. J. Cismowski, and S. E. Hamrick. 2014. Cytokine levels in the preterm infant with neonatal intestinal injury. *Am. J. Perinatol.* 31: 489–496.
75. Murgas Torrazza, R., N. Li, C. Young, F. Kobeissy, M. Chow, S. Chen, V. Mai, R. Sharma, M. Hudak, J. Shuster, and J. Neu. 2013. Pilot study using proteomics to identify predictive biomarkers of necrotizing enterocolitis from buccal swabs in very low birth weight infants. *Neonatology* 104: 234–242.
76. Niinikoski, H., B. Stoll, X. Guan, K. Kansagra, B. D. Lambert, J. Stephens, B. Hartmann, J. J. Holst, and D. G. Burrin. 2004. Onset of small intestinal atrophy is associated with reduced intestinal blood flow in TPN-fed neonatal piglets. *J. Nutr.* 134: 1467–1474.
77. Ganessunker, D., H. R. Gaskins, F. A. Zuckermann, and S. M. Donovan. 1999. Total parenteral nutrition alters molecular and cellular indices of intestinal inflammation in neonatal piglets. *JPEN J. Parenter. Enteral Nutr.* 23: 337–344.
78. Wullaert, A., M. C. Bonnet, and M. Pasparakis. 2011. NF-κB in the regulation of epithelial homeostasis and inflammation. *Cell Res.* 21: 146–158.
79. Toti, P., and C. De Felice. 2001. Chorioamnionitis and fetal/neonatal brain injury. *Biol. Neonate* 79: 201–204.
80. Chau, V., D. E. McFadden, K. J. Poskitt, and S. P. Miller. 2014. Chorioamnionitis in the pathogenesis of brain injury in preterm infants. *Clin. Perinatol.* 41: 83–103.
81. Allan, S. M., and E. Pinteaux. 2003. The interleukin-1 system: an attractive and viable therapeutic target in neurodegenerative disease. *Curr. Drug Targets CNS Neurol. Disord.* 2: 293–302.
82. Pickler, R., L. Brown, J. McGrath, D. Lyon, D. Rattican, C. Y. Cheng, L. Howland, and N. Jallo. 2010. Integrated review of cytokines in maternal, cord, and newborn blood: part II—associations with early infection and increased risk of neurologic damage in preterm infants. *Biol. Res. Nurs.* 11: 377–386.
83. Kermorvant-Duchemin, E., F. Sennlaub, M. Sirinyan, S. Brault, G. Andelfinger, A. Kooli, S. Germain, H. Ong, P. d'Orleans-Juste, F. Gobeil, Jr., et al. 2005. *Trans*-arachidonic acids generated during nitrative stress induce a thrombospondin-1-dependent microvascular degeneration. *Nat. Med.* 11: 1339–1345.
84. Sirinyan, M., F. Sennlaub, A. Dorfman, P. Sapieha, F. Gobeil, Jr., P. Hardy, P. Lachapelle, and S. Chemtob. 2006. Hyperoxic exposure leads to nitrative stress and ensuing microvascular degeneration and diminished brain mass and function in the immature subject. *Stroke* 37: 2807–2815.
85. González-Frankenberger, B., T. Harmony, J. Ricardo-Garcell, E. Porras-Kattz, A. Fernández-Bouzas, E. Santiago, and G. Avecilla-Ramírez. 2008. Habituation of visual evoked potentials in healthy infants and in infants with periventricular leukomalacia. *Clin. Neurophysiol.* 119: 2879–2886.
86. Girard, S., L. Tremblay, M. Lepage, and G. Sébire. 2010. IL-1 receptor antagonist protects against placental and neurodevelopmental defects induced by maternal inflammation. *J. Immunol.* 184: 3997–4005.
87. Wu, Y. W., G. J. Escobar, J. K. Grether, L. A. Croen, J. D. Greene, and T. B. Newman. 2003. Chorioamnionitis and cerebral palsy in term and near-term infants. *JAMA* 290: 2677–2684.
88. Burd, I., A. I. Bentz, J. Chai, J. Gonzalez, H. Monnerie, P. D. Le Roux, A. S. Cohen, M. Yudkoff, and M. A. Elovitz. 2010. Inflammation-induced preterm birth alters neuronal morphology in the mouse fetal brain. *J. Neurosci. Res.* 88: 1872–1881.
89. Elovitz, M. A., A. G. Brown, K. Breen, L. Anton, M. Maubert, and I. Burd. 2011. Intrauterine inflammation, insufficient to induce parturition, still evokes fetal and neonatal brain injury. *Int. J. Dev. Neurosci.* 29: 663–671.
90. Burd, I., A. Brown, J. M. Gonzalez, J. Chai, and M. A. Elovitz. 2011. A mouse model of term chorioamnionitis: unraveling causes of adverse neurological outcomes. *Reprod. Sci.* 18: 900–907.
91. Impey, L. W., C. E. Greenwood, R. S. Black, P. S. Yeh, O. Sheil, and P. Doyle. 2008. The relationship between intrapartum maternal fever and neonatal acidosis as risk factors for neonatal encephalopathy. *Am. J. Obstet. Gynecol.* 198: 49.e1–49.e6.
92. Becroft, D. M., J. M. Thompson, and E. A. Mitchell. 2010. Placental chorioamnionitis at term: epidemiology and follow-up in childhood. *Pediatr. Dev. Pathol.* 13: 282–290.
93. Grether, J. K., and K. B. Nelson. 1997. Maternal infection and cerebral palsy in infants of normal birth weight. *JAMA* 278: 207–211.
94. Wu, Y. W., L. A. Croen, S. J. Shah, T. B. Newman, and D. V. Najjar. 2006. Cerebral palsy in a term population: risk factors and neuroimaging findings. *Pediatrics* 118: 690–697.
95. Kenakin, T. 2014. *A Pharmacology Primer: Techniques for More Effective and Strategic Drug Discovery*, 4th Ed. Academic Press, San Diego, CA.
96. Girard, S., and G. Sebire. 2016. Transplacental transfer of interleukin-1 receptor agonist and antagonist following maternal immune activation. *Am. J. Reprod. Immunol.* 75: 8–12.